1964ApJ...140.1120S

VELOCITY FIELDS IN THE SOLAR ATMOSPHERE. III. LARGE-SCALE MOTIONS, THE CHROMOSPHERIC NETWORK, AND MAGNETIC FIELDS*

G. W. SIMON† AND R. B. LEIGHTON
California Institute of Technology, Pasadena, California
Received March 23, 1964; revised May 4, 1964

ABSTRACT

Results of a detailed study of large-scale cellular motions in the solar photosphere are presented. The velocity cells (called "supergranules") are of various sizes and shapes and have an average diameter of 32000 km and a 20-hour lifetime; the motion within each cell is mainly horizontal, proceeding from the center toward the outer boundary with a velocity of 0.3–0.5 km/sec. A strong spatial correspondence is found between the cell boundaries and several other features: (1) the chromospheric Ca^+ λ 3934 network; (2) the network of descending matter (1.0–2.0 km/sec) observed in Hα and Hβ; and (3) the magnetic field pattern. The characteristics of the velocity cells suggest that they are non-stationary convection currents originating perhaps at a quite deep level inside the convective envelope. These observations, together with the theoretical predictions of Parker (1963*a*, *b*) and Osterbrock (1961), suggest an explanation for the origin of the chromospheric network seen in Ca^+ and in the Balmer lines

I. INTRODUCTION

As previously reported (Leighton, Noyes, and Simon 1962, hereinafter called Paper I; Simon and Leighton 1963), large-scale, cellular, horizontal motions have been observed in the solar photosphere. The preliminary observations reported in Paper I indicated a qualitative correspondence between these "large cells," or "supergranulation"[1] and various other solar phenomena: the bright emission network seen in Ca^+ K_{232} spectroheliograms, a system of predominantly downward-moving columns of gas in the low chromosphere, and the distribution of magnetic fields on the surface of the quiet Sun. In the present paper we shall describe the results of a more detailed and quantitative analysis of the supergranulation and its relation to the above-mentioned phenomena. These new results confirm the earlier ones and permit the construction of a plausible and consistent picture of several large-scale phenomena which exist in the atmosphere of the quiet Sun.

In the following sections we shall describe modifications of the apparatus, some new observations, methods of data analysis, the results of this analysis, and finally, a discussion of the results in light of previous observational and theoretical work in this field.

II. APPARATUS

The observational techniques and measurement procedures are the same as were described in Paper I except that, in addition to the equipment previously described, three further pieces of apparatus were used extensively in the present observations and analysis.

A new telescope system, utilizing a concave mirror of 9.0-m focal length and 25-cm aperture, was installed in the Mount Wilson 20-m solar tower. This objective produces a solar image 8.4-cm in diameter; when used in conjunction with the beam splitter and line shifter, this enables the observer to take simultaneous side-by-side full-disk images

* Assisted in part by the Office of Naval Research.

† Now at Sacramento Peak Observatory, Sunspot, New Mexico.

[1] The resemblance of these motions to those associated with non-stationary cellular convection led us to suggest the name "supergranulation" to describe them, in analogy to the ordinary photospheric granulation.

© American Astronomical Society • Provided by the NASA Astrophysics Data System

1964ApJ...140.1120S

of the Sun in two wavelengths. Although this was also possible with the 5-cm image previously available, the resolution and quality of the large image is considerably better.

Second, the autocorrelation device described in Paper I was modified to permit azimuthal scans (parallel to the limb of the Sun) by slowly rotating one plate with respect to the other. With this arrangement it is possible to obtain correlation data for a series of narrow concentric annular rings, and thus easily to study changes in phenomena from the center of the disk to the limb.

Finally, in projection printing right-left pairs of plates to be analyzed by the correlation device, a 25-cm focal length plano-convex condensing lens was often placed in the optical path directly above the photographic emulsion. This introduced pin-cushion distortion which largely compensated for the barrel-like distortion of elements on the Sun due to geometrical foreshortening. As a result of this procedure it was possible to "flatten out" rather large areas near the center of the Sun, and thus to follow features for 4–5 days without appreciable distortion.

III. OBSERVATIONS

With the exception of a few 1961 plates, the observations reported in this paper were made during the summer of 1962. Photographs were generally taken during periods of very good atmospheric seeing beginning shortly after sunrise and continuing for up to 2 hours. However, in the study of the Ca^+ network lifetime, spectroheliograms were taken at 2–12-hour intervals over a 50-hour period, whenever the Sun was visible, regardless of seeing conditions.

The long-lived supergranulation velocity field was studied by means of "Doppler-sum" plates in which the two sets of images were taken 2–3 min apart, using the 8.4-cm image. Ideally, the time difference should be 150 sec in order to minimize the signal contributed by the small-scale granulation motions which have an oscillation period of 5 min (Paper I). Spectroheliograms were taken in Ca 6103, Ba^+ 4554, and Na 5896.

To observe the chromospheric network the lines $H\alpha$, $H\beta$, $H\gamma$ and Ca^+ 3934 were used, generally using the 17-cm solar image.

Magnetic fields were observed both by the method of Leighton (1959), and by a new scheme carried out in collaboration with Dr. R. Howard using the magnetograph in the 150-foot solar telescope at Mount Wilson. This latter technique was designed to indicate directly any existing spatial correspondence between Ca^+ emission and magnetic fields: The two exit slits of the spectrograph were separated by 25.7 mm so that the Zeeman-sensitive Fe 5250 line was centered on one exit slit in third order, and the Ca^+ 3934 line was centered on the other exit slit in fourth order. With a fourth-order dispersion of 0.21 Å/mm, the second slit width of 2.3 mm corresponded to a wavelength spread $\Delta\lambda = 0.48$ Å, which is roughly the width of the K_{232} emission peak, The light emerging through this slit passed through a deep blue filter, and thence to a 931-A photomultiplier tube and amplifier. The light from the first exit slit was treated in the usual magnetographic fashion, set in the magnetic mode. The aperture for the incident light was a rectangle $10'' \times 18''$, located near the center of the 40-cm solar image. The magnetic signal was fed into the Y channel and the K_{232} emission signal into the X channel of an X-Y recorder. (In addition, each signal was separately measured on a strip-chart recorder.) A correlation between the Ca^+ emission and magnetic field intensity should then show up as a motion of the X-Y recorder pen away from both the X- and Y-axes.

Finally, the magnetograms and Ca^+ spectroheliograms obtained by Howard (1959) on September 3 and 5, 1958 were used in the present work.

IV. ANALYSIS PROCEDURES

Many of the results reported in the following sections were obtained by the correlation techniques described in Paper I. Auto-correlation (AC) curves of a spatially fluctuating field furnish directly two important pieces of information about that field: the

© American Astronomical Society • Provided by the NASA Astrophysics Data System

1964ApJ...140.1120S

full width at half-maximum (FWHM) is a measure of the "correlation distance" or the linear scale of the fluctuations, and the central height (H) is a measure of the r.m.s. fluctuation. In the case of the essentially random velocity field associated with the small-scale granulation it is relatively easy, by such statistical treatment, to interpret the height H in terms of an r.m.s. velocity on the Sun. However, in the case of the supergranulation, each cell is more nearly a separate entity with a characteristic velocity pattern, and it is necessary to consider in more detail the relationship between H and the actual velocity field on the Sun. Similar remarks apply even more to cross-correlation (CC) curves between different phenomena, such as the supergranulation versus the Ca^+ network.

We have found it instructive to consider the properties of a simple analytical model of the velocity and intensity fields. For example, let us suppose that it is possible to describe the velocity in a typical cell by $V(\rho)$, where ρ is the radius vector of a plane-polar coordinate system in the solar surface with origin at the center of the cell. The line-of-sight velocity component V_L observed at an angle θ from the vertical is then

$$V_L(x, y) = \frac{y \sin \theta}{\rho \cos \theta} F_h(\rho) + \cos \theta F_v(\rho), \tag{1}$$

where (x, y) are rectangular coordinates on the photographic plate with x parallel to the solar limb, and $F_h(\rho)$ and $F_v(\rho)$ are the horizontal and vertical components of $V(\rho)$. Note that $x^2 + y^2/\cos^2 \theta = \rho^2$ because of geometrical foreshortening.

We do not know, of course, the form of the functions F_h and F_v, and these are in any case primarily of statistical significance. However, we saw in Paper I that the major features of auto-correlation curves are rather insensitive to the exact shape of the function in the integrand; we shall use functions quite similar to those used by Pellew and Southwell (1940) to describe the velocities in hexagonal convection cells, although, of course, their idealized convection model with fixed boundary conditions is certainly not a proper description of the complex solar phenomenon we are observing. These functions are

$$F_h(\rho) = V_h \sin (2\pi\rho/L) \tag{2}$$

and

$$F_v(\rho) = \frac{2V_v}{3}(S^2 + S - 0.5), \tag{3}$$

where $S = \cos (4\pi\rho/3L)$ and L is the cell diameter.

By using this model of a supergranule, together with the equations developed in Paper I, namely:

$$\delta(\rho) = \frac{\lambda V_L(\rho)}{I_0 c} \frac{dI}{d\lambda}, \tag{4}$$

and

$$I(\rho) = I_0 [1 + \delta(\rho)], \tag{5}$$

we can then easily calculate the correlation function

$$C(s, t) = \frac{K}{A} \iint T_1(x, y) T_2(x + s, y + t)\, dA, \tag{6}$$

since the transmission $T(\rho)$ of a Doppler-sum plate is related to the intensity of light passing through the spectroheliograph slits by

$$T(\rho) = T_0 \left[\frac{1 \pm \delta(\rho)}{1 \mp \delta(\rho)}\right]^{2\Gamma}, \tag{7}$$

© American Astronomical Society • Provided by the NASA Astrophysics Data System

1964ApJ...140.1120S

where Γ is the contrast of the original plate. The function $C(s, t)$ (calculated by numerical integration on an IBM 7090 computer) then gives us a basis for interpreting the height H of the AC function of the actual supergranulation field in terms of an "average" velocity $V_L(\rho)$.

In analogy to equations (2) and (3), which describe the velocity field in a large cell, simple models were also devised to describe the network pattern of Ca^+ emission and downward flowing material seen in Hα, Hβ, and Hγ. For example, in the Ca^+ case, we assumed a function

$$T(\rho) = T_0 [1 + \sin \pi(2\rho/R + 1)] \; 0.5 < \rho/R < 1.0 ,$$
$$T(\rho) = T_0, \text{ elsewhere.} \tag{8}$$

This function describes an annular intensity field which has a maximum at $\rho_0 = 0.75$ $R = 0.5$ L, where L is the cell diameter.

From such models it was possible to predict the approximate shapes of AC and CC curves, and to compare them with the actual tracings obtained from spectroheliograms.

To measure the lifetime of the Ca^+ network, we define a normalized time-correlation function $F(\Delta t)$ of two plates taken at times t_1 and t_2:

$$F(\Delta t) = \frac{H_{cc}(\Delta t)}{[H_{ac}(t_1) \times H_{ac}(t_2)]^{1/2}}, \tag{9}$$

where $\Delta t = t_2 - t_1$, H_{cc} is the CC height, and $H_{ac}(t_1)$, and $H_{ac}(t_2)$ the AC heights of the two plates.

In addition to the above correlation methods, in some instances we compared drawings, rather than spectroheliograms, of the pertinent solar features. In these cases, we counted the number (C) of features which correlated out of the total number (N) observed, and compared this with the number expected from random fluctuations of uncorrelated fields, which is given by the cumulative binomial probability $E(C; N, P)$.

V. RESULTS

a) Geometrical Properties of the Supergranulation

In this section we describe measurements directed toward establishing the quantitative properties of the supergranulation velocity field: its amplitude, cell size, and organization. We first summarize briefly the principal qualitative features seen on a typical large cell (LC) Doppler-sum photograph:

1. The solar surface is covered rather uniformly by a cellular system of moving material.

2. The cells are virtually indistinguishable from the background of small-scale motions at the center of the disk, implying that the velocity field consists mostly of *horizontal* motions. Upon close inspection of a few of the best quality Doppler-sum plates, one also sees at the center of the disk a *very faint* pattern of rising velocities at the center of each cell, and a network of descending motions at the cell boundaries.

3. Away from the center of the disk, most of the individual cells, which range from roughly 20000 to 50000 km in size, have a definite "polarity": the line-of-sight motion in a cell is one of recession on the side nearer the limb, and of approach on the side nearer the center of the disk.

4. In general, the cells appear elongated parallel to the limb, as if seen in projection. If the cells were visible at the disk center, they would presumably have an irregularly circular or perhaps polygonal form.

5. The velocity pattern has a lifetime of several hours.

From such observations we have inferred the existence of a system of essentially horizontal currents on the Sun, distributed in cells a few tens of thousands of kilometers in

© American Astronomical Society • Provided by the NASA Astrophysics Data System

1964ApJ...140.1120S

diameter, with the motion in each cell proceeding from the center toward the outer boundary.

In order to make a quantitative comparison between the actual velocity field and the supergranule model represented by equations (2) and (3), actual microphotometer scans were made across the center of a number of large cells, in a direction perpendicular to the limb. One of these is shown in Figure 1. These were in excellent agreement with the expected sinusoidal variation given in equation (2). If we define D as the distance on the Sun between the two peaks in the velocity distribution, then we would expect the cell size L to be approximately twice D. Results of forty-five microphotometer scans yielded an average distance $\langle D \rangle = (12.9 \pm 0.4) \times 10^3$ km and an average peak velocity $\langle V_h \rangle = 0.42 \pm 0.13$ km/sec, where the errors are standard deviations in the mean. A few faint structures were found near the center of the disk on the best LC plate studied, which appeared to show cores of rising material and narrow boundaries of falling material. Microphotometer tracings across four such objects yielded velocities V_v of 0.13–0.30 km/sec with an average of 0.20 km/sec. If these are indeed large cells, then it would seem that the vertical velocity in a cell in general does not exceed about 50 per cent of the horizontal components, and is usually much smaller than this.

To increase the statistical precision of the measurements, the large cells were next analyzed by auto-correlation techniques. Six 8.4-cm LC plates were studied; on each plate 27 AC curves were made at thirteen different radial positions, the field of view consisting of annular openings with widths corresponding to distances of 120000–170000 km on the Sun. Fourteen of the scans on each plate were made perpendicular to the solar limb (the y-direction), the others parallel to the limb. A complete annulus was used for the "parallel" scans, but only a 40° sector centered on the y-axis was open for the "perpendicular" tracings. A typical pair of actual AC scans is shown in Figure 2. These illustrate three striking differences between the appearance of scans made parallel and perpendicular to the limb, at the same place on a single image of the sun: (1) the height of the perpendicular scan exceeds that of the parallel scan by about 40 per cent (in good agreement with the theoretical AC functions of Paper I for which the excess was 50 per cent); (2) the width (FWHM) of the perpendicular-scan curve is smaller than that of the parallel-scan curve, though the difference is smaller than predicted by the model functions; and (3) secondary maxima are present in the perpendicular scans.

Two methods were used to determine the cell size. First, for each value of $\sin \theta$ an average FWHM from the six plates was calculated, as plotted in Figure 3. The steady decrease in FWHM as $\theta \rightarrow 0$ is an effect of the superposition of the large-scale, mainly horizontal motion and the small-scale, mainly vertical oscillatory motions discussed by Noyes and Leighton (1963). Near the limb, the small-scale motion nearly disappears, so that the remaining FWHM is due primarily to the large-scale motion. A least-squares straight-line fit to this data gives a FWHM at $\theta = 90°$ of 15.3×10^3 km and 16.2×10^3 km for the perpendicular and parallel scans, respectively. Using the theoretical relationship between FWHM and the cell size L as obtained from equation (2), we then deduce an average cell size to 30.0×10^3 km. It should be noted that the FWHM values quoted above agree very well with those in Paper I. However, an error was made in Paper I in equating the FWHM to the cell size. The subsequent analysis of AC functions indicates that $L \approx 2$ FWHM is more representative of the cell size. For example, using the supergranule model described by equation (2), we find that equation (6) yields the relations $L = 2.27$ FWHM and $L = 1.56$ FWHM for perpendicular and parallel scans, respectively.

The secondary maxima of Figure 2, *b*, imply some sort of periodicity or local order in the cell structure, and we can therefore determine the cell size[2] L by measuring

[2] Cell "spacing" would be a more accurate description; however, in Paper I, we showed from a count of the number of cells on the solar surface that they are effectively close-packed, so that "spacing" and "size" are interchangeable.

© American Astronomical Society • Provided by the NASA Astrophysics Data System

1964ApJ...140.1120S

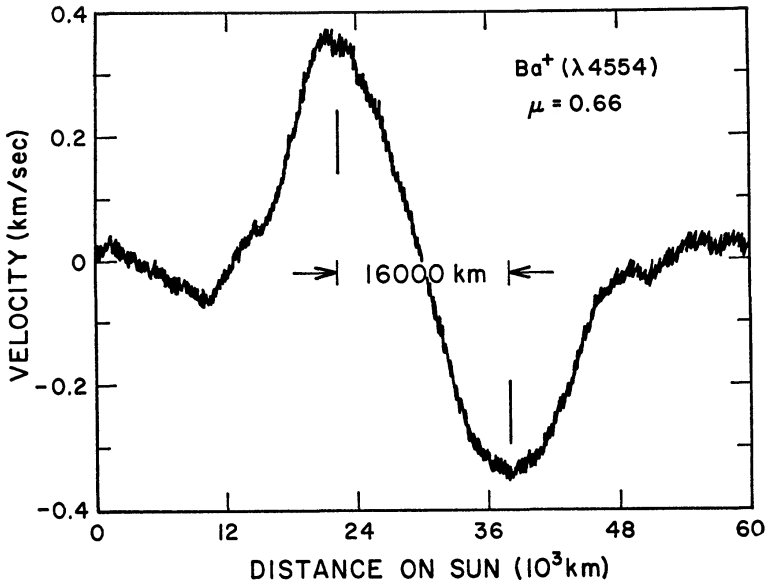

FIG 1 —Microphotometer tracing across a large cell, from Doppler sum plate of June 23, 1963

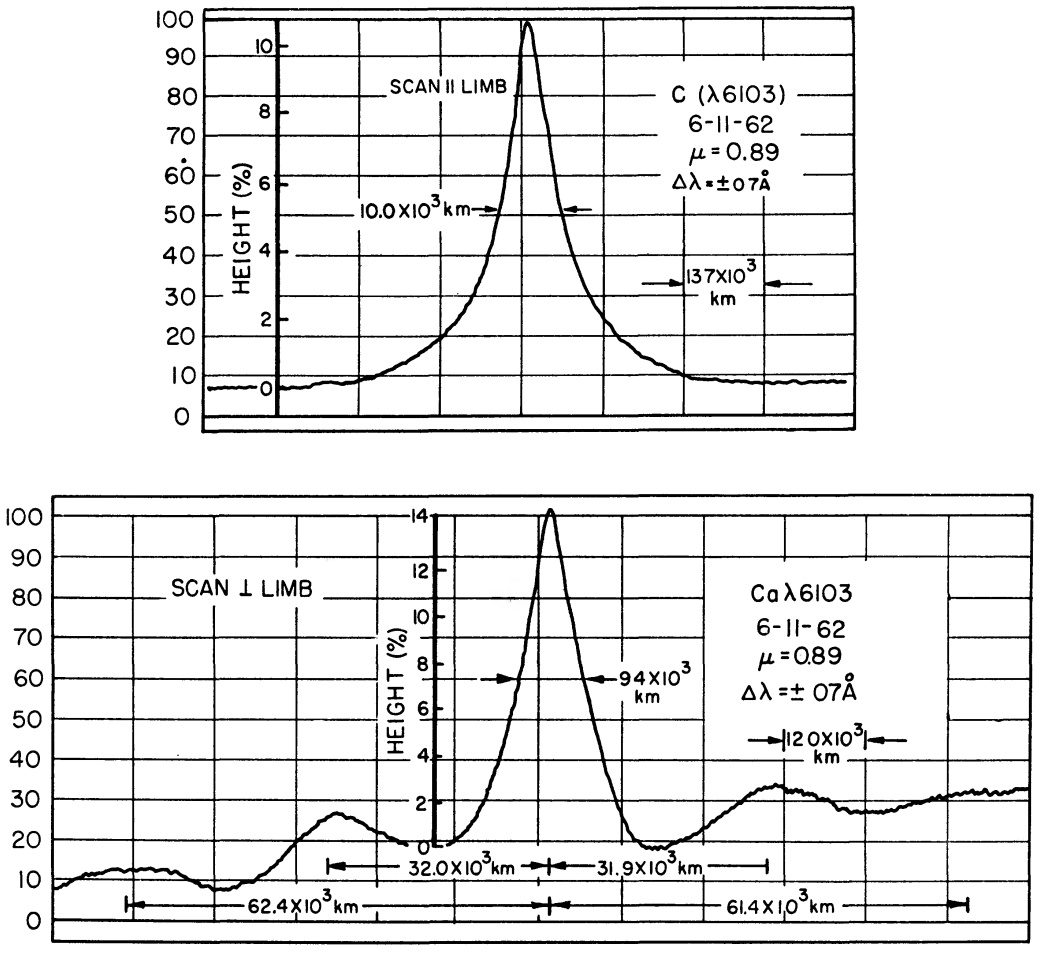

FIG. 2.—Actual tracing of an AC function of large cells on June 11, 1962. Scan parallel to limb (*above*) and perpendicular to limb (*below*). Note secondary maxima at 32×10^3 km and 62×10^3 km.

© American Astronomical Society • Provided by the NASA Astrophysics Data System

1964ApJ...140.1120S

the distances corresponding to the subsidiary peaks. In Figure 4 we have plotted the distribution of the distances to the first subsidiary maximum for 132 measurements of AC tracings from the six plates studied. The average value of L by this method is $(32.5 \pm 0.65) \times 10^3$ km, where the error is the standard deviation of the mean.[3] The observed values of L range from 20000 to 54000 km, indicating that there exists a large spread in cell sizes; we are not yet certain as to the reason for this variability in the periodicity of the cell spacing.

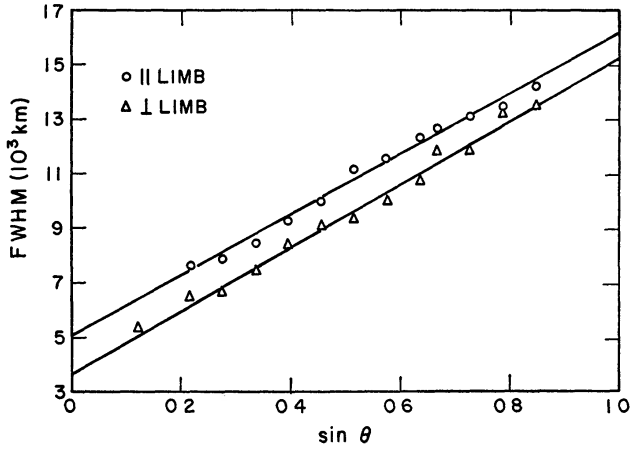

FIG. 3.—Composite curve of FWHM versus sin θ for six large-cell plates

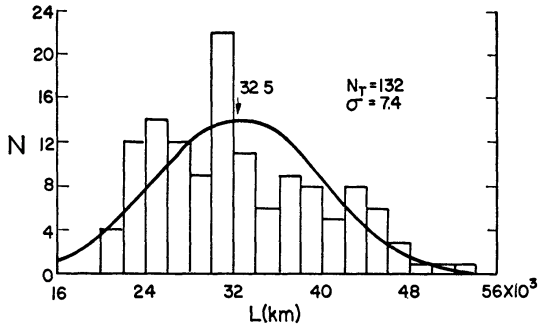

FIG. 4.—Distribution of distance L to first subsidiary maxima on large-cell AC curves

From the heights of the AC curves, we can calculate the velocity of the cell motion according to the method described in Section IV. On this basis we find an average peak velocity of 0.35 km/sec, slightly less than from the direct microphotometer tracings. This is to be expected, since the AC function is integrated over many cells, while the direct tracings were made across a few chosen cells which clearly had a "proper" cell appearance, and particularly good contrast (i.e., large velocity) between the dark and light halves of the cell.

There still exists the problem of vertical motions in large cells, which would be given by the height (H) of an AC curve obtained at the center of the disk. Unfortunately, the oscillating small-scale field is also present, and this contributes a tall, narrow peak to the AC curves. We have tried to eliminate this by forming Doppler sums from plates

[3] The smooth curves in Figs. 4 and 7 are normal distributions whose mean values and standard deviations are the same as those of the actual data.

© American Astronomical Society • Provided by the NASA Astrophysics Data System

1964ApJ...140.1120S

taken half an oscillation period apart, so that the small-scale contrast is at a minimum, by using the 8.4-cm image which has poorer resolution than the 17-cm image, and finally by slight defocusing of the image. However, some of the granular motion inevitably remains and is inseparably mixed with the large-cell vertical motion. Thus it is not possible to interpret H at the center of the disk except qualitatively. The average AC height obtained from the six plates at the center of the disk is about 55 per cent of the height at the limb. Since the r.m.s. velocity goes roughly as the square root of the AC height, this would imply vertical velocities about 75 per cent of the horizontal velocities. Thus the upper limit for the vertical-cell velocity is about 0.25 km/sec, assuming none of the height is due to the granulation field. Of course, this is not true, as can be seen by examining the plates themselves. Indeed, it is much more likely that the center-of-the-disk height is due primarily to the small-scale motion, since we recall that the FWHM in Figure 3 decreased sharply as we approach the center of the disk.

b) Correlation between the Large Cells and the Ca^+ Network

Immediately after discovery of the large cells, it was noticed that a rather strong moiré pattern could be produced by superimposing a velocity plate upon an ordinary Ca^+ K-line spectroheliogram, and sliding one plate slowly across the other. This moiré pattern usually persists even for displacements of from two to four cell diameters, and is seen even if the two plates were taken several hours apart. Not only did this indicate a geometrical relationship between the two phenomena, but also at least a quasi-periodicity in the observed structures, and a relatively long lifetime, perhaps many hours. In this section we shall describe two methods which were used to establish that the boundaries of the large cells seen on Doppler plates do in fact correspond to the emission network visible in the K_2 or K_3 spectroheliograms. We shall subsequently discuss the periodicity and lifetime of the network, respectively, in the following two sections.

1. *Correlation by counting individual cells.*—Our first successful attempt to measure quantitatively the correlation between the K-network and the large cells (henceforth called "K-LC correlation") was made as follows: An 8.4-cm K-plate was placed in an enlarger and projected as a 46-cm image on a sheet of white paper, and a drawing was made of the emission network. Then an 8.4-cm LC plate, taken within an hour or so of the K-plate, was enlarged to the same scale, and a drawing made of all structures which appeared as cells to the viewer.[4] One observer then placed the two drawings in register and made four sets of identifying marks, one with the drawings in proper registration and three others with one drawing rotated through successive 90° intervals. A second observer, who did not know which set of marks corresponded to the correct alignment, then measured the K-LC correlation for all four orientations of the two drawings in the following manner. The two figures were placed on a light box. Each cell on the LC drawing was assigned a letter "C" or "A." A value "C" indicated that the cell "correlated"; i.e., it lay entirely within or just touched the inner boundary of a K-network polygon; an assignment "A" meant "anticorrelation"; i.e., the cell was intersected by one or more pieces of the K-network structure. A few cells, though not intersected by the K-network, were not counted as C, if they were a large distance (roughly more than one cell diameter) away from the nearest network piece. These cells were thrown out. This procedure was carried out twice (to check the observer's consistency of judgment) for each of the four orientations, and for four pairs of drawings. Two of the LC drawings were made from Ca 6103 plates; two used Ba^+ 4554.

For each pair of drawings, the three "wrong-alignment" positions measured the probability P that a randomly placed, uncorrelated cell would appear as a "C" cell. The probability that at least C correlations would be observed in N trials, if the distribution

[4] To qualify as a cell, the object had to have the "right" polarity; i.e., receding velocity in the half of the cell nearer the limb of the Sun.

© American Astronomical Society • Provided by the NASA Astrophysics Data System

1964ApJ...140.1120S

of cells were completely random, (i.e., uncorrelated with the K-network) is given by the cumulative binomial probability $E(C; N, P)$. For the four pairs of drawings investigated, the results are shown in Table 1.

Looking first at Cases 1–3, each of which involved plates with time differences less than 1 hour, one is immediately struck by the extremely small probability E that the measured correlation is due to random statistical fluctuations in the cell-network distribution.

However, in Case 4, one notes that the ratio C/N is actually less than P. That is, the cells in Case 4 appear to be *anticorrelated* with the K-network. This is also indicated by the large value of E, which is over 90 per cent. The 96-min time interval between the plates probably explains the discrepancy for this case. In 96 min, objects within 40° or so from the solar equator will move roughly 10000 km across the surface. This is approximately $\frac{1}{3}$ the average cell diameter; thus many of the cells which correlated with the K-network at $\Delta t = 0$ will now have moved enough to be intersected by segments of the K-network.

TABLE 1

CORRELATIONS OF LARGE CELLS WITH THE CHROMOSPHERIC NETWORK

Case	Type	Date	Δt	N	C	P	C/N	E
1	Ca-K	6/27/62	12^m	492	387	0 540	0 786	3×10^{-22}
2	Ba-K	6/23/62	36	394	231	511	587	4×10^{-3}
3	Ca-K	6/22/62	49	275	185	482	672	3×10^{-10}
4	Ba-K	7/ 2/62	96	674	386	0 603	0 573	0 92

Concerning the significance of the calculated values of E, which are seen to vary tremendously from case to case, the precise measured values of E must not be taken too seriously.[5] However, their small size demonstrates that a very strong correlation exists between the large cells and the Ca^+ network, such that the velocity cells are *inclosed* by the polygonal structure of the K-network, rather than *intersected* by it.

2. *Correlation from direct cross-correlation measurements.*—Since the above method clearly established the spatial correspondence of the cell boundaries and the K-network, a new effort was made to verify this correspondence directly using cross-correlation measurements, without recourse to an intermediate stage involving drawings. A similar attempt had failed in 1961 because of the great difficulty in properly aligning the two plates (17-cm Doppler plates generally do not show opposite limbs of the Sun). This problem was eliminated through use of the new 8.4-cm full-disk Doppler images available in 1962.

To see how a K-LC cross-correlation function should appear, consider the very schematic one-dimensional drawing of a superposition of the velocity cells and the K-network (shown in Fig. 5, *a*). Three typical cases of cells are shown, one at the center of the disk, and one each on the "left" and "right" side of the disk, as seen by the observer. The dashed lines refer to the plate transmission of the K-emission network, the solid lines to that of the velocity field (assumed to arise mainly from horizontal motions in the left and right cells, and from vertical motions at the center). The horizontal axis represents displacement along the solar surface, and the vertical axis, transmission through the plates (referred to the mean transmission). In the plates studied, the Doppler polarities were such that both the K-network and receding line-of-sight velocities appeared as higher-than-average transmission.

[5] For example, in Case 3 above, if the observer had counted 183 or 187 C's instead of 185, the respective probabilities would have been $E = 1 \times 10^{-9}$ and $E = 5 \times 10^{-11}$.

© American Astronomical Society • Provided by the NASA Astrophysics Data System

1964ApJ...140.1120S

Consider the CC functions for the three local regions at the left side, right side, and center of the disk. A displacement of the left velocity cells toward the left relative to the K-plate by an amount C, or of the right cells toward the right by a similar distance, should produce a relative maximum in the corresponding cross-correlation functions, because high-transmission regions on the two plates would then coincide. Conversely, a displacement of the left cell toward the right, or the right one toward the left, would superimpose dark regions upon light ones, and would thus result in a relative minimum in the cross-correlation function. Both of these effects could easily be seen visually when

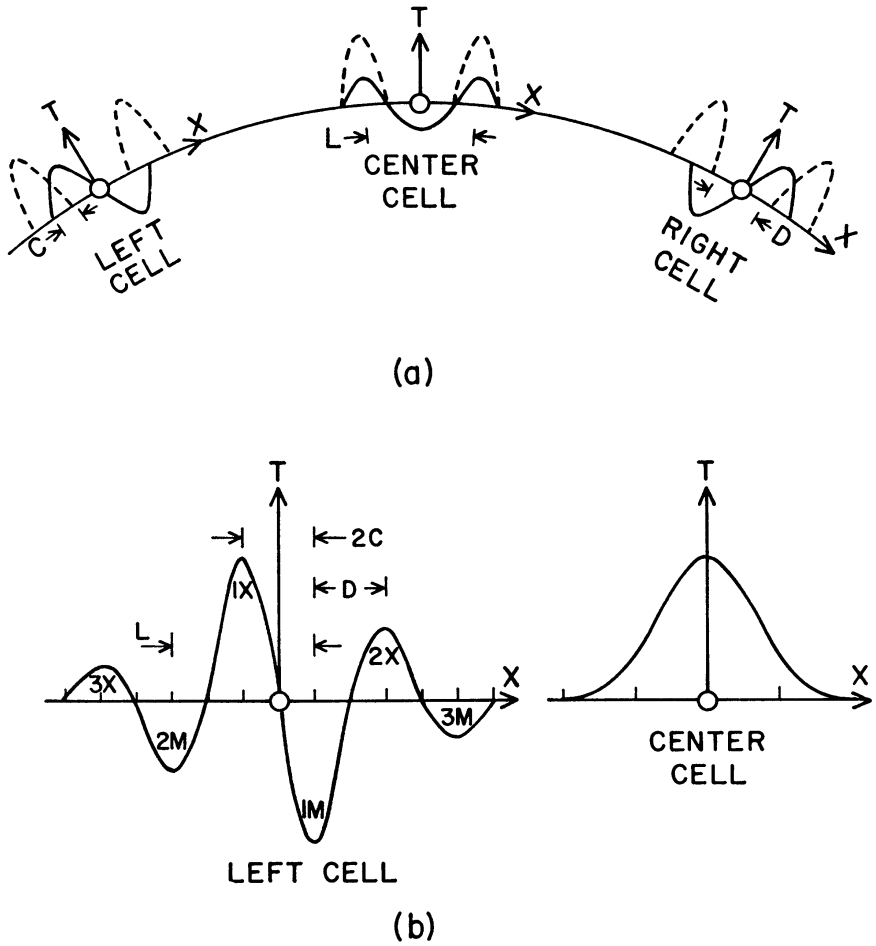

FIG. 5.—Schematic model showing correlation between Ca^+ network and large cells

two such plates were superimposed, especially the transmission minimum, which appeared as a rather featureless gray field. At the center of the disk, where we assume that the motion is upward at the cell center and downward at the edges, one would expect a relative maximum at zero displacement. With the naked eye it was extremely difficult to detect more than a faint hint that such a maximum might exist, demonstrating again that the vertical-cell motion is either very small or masked by the small-scale oscillating field.

These expected relative maxima and minima in the cross-correlation function are shown schematically in Figure 5, *b:* The left-hand curve refers to cells at the left side of the disk, and the right-hand curve to cells at the disk center. (The CC function for the

© American Astronomical Society • Provided by the NASA Astrophysics Data System

1964ApJ...140.1120S

right side is of course just the reverse of that for the left.) In the left-hand sketch, a series of successive maxima ($1X$, $2X$, $3X$) and minima ($1M$, $2M$, $3M$) is shown. Whether all of these peaks actually appear depends on the regularity of the velocity cell and K-network spacing. If we define the distance (in Fig. 5, *a*) between the velocity cell maximum and minimum as D, and the cell size as L, then the cross-correlation curve in Figure 5, *b* (*left*), measures various distances which are combinations of D, L, and $C = (L - D)/2$. If all six of the drawn peaks exist, then fifteen such combinations can be measured in a single CC run, thus providing a wealth of statistical information from a relatively small number of tracings. (Compare this to a typical A-C run, which gives but one measurement of L, and one of the FWHM, a quantity roughly equal to D.)

Such cross-correlations were measured on three pairs of Ca 6103 and Ca^+ 3934 plates. A typical CC tracing for a right-hand cell is shown in Figure 6, *a*. Note the similarity between this actual tracing and the schematic model of Figure 5, *b* (*left*), with $x = 0$ occurring *between* $1M$ and $1X$. Tracings across left (right)-hand cells were made at ten different radii, each 0.5 cm wide (on the 8.4-cm diameter image), by masking out all of the annulus except a narrow sector of 40° on the left (right) side of the image. The open

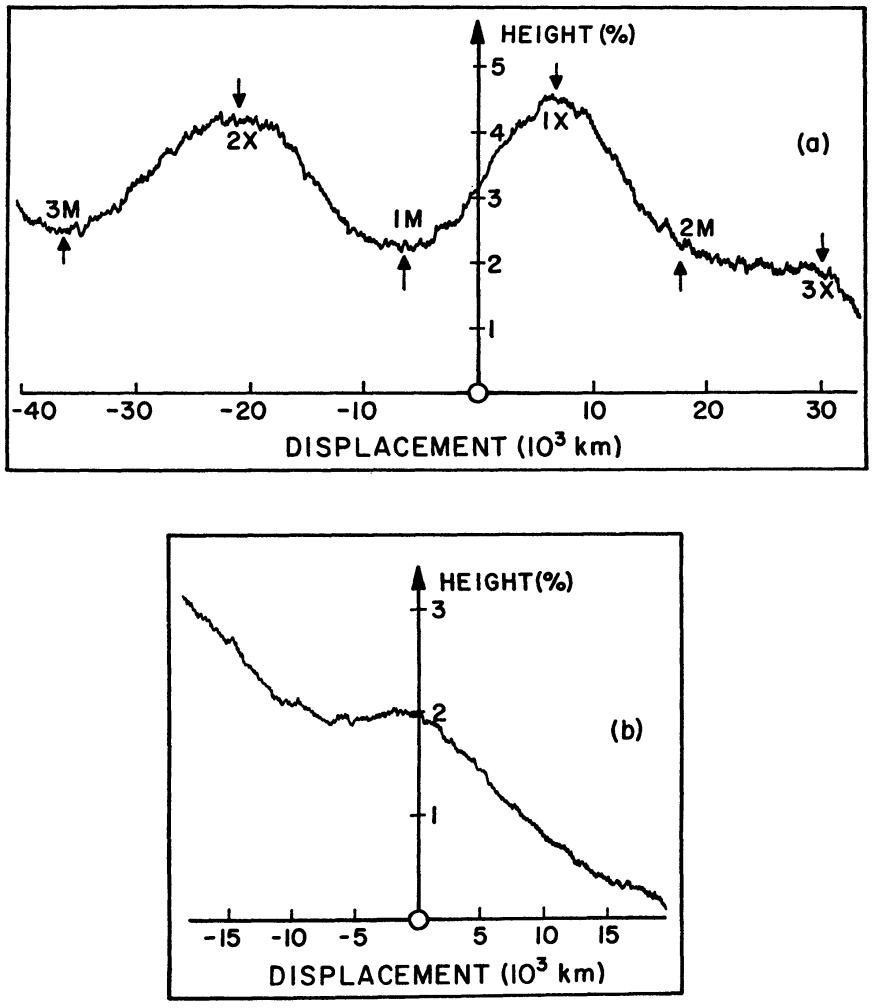

FIG. 6.—Actual tracings of CC functions between Ca^+ and large cells. (*a*) Scan across "right-hand" cell, (*b*) across a cell at center of disk.

© American Astronomical Society • Provided by the NASA Astrophysics Data System

1964ApJ...140.1120S

sector was centered on the x-axis; i.e., along the direction of scan, which was perpendicular to the limb of the Sun. For each left and right tracing, the plate displacements corresponding to all major maxima and minima were recorded. These data, along with the value of μ, were analyzed on an IBM 7090 computer, using a program which corrected for geometrical foreshortening, transformed the plate offsets into kilometers on the Sun and combined the results by a least-squares analysis. The results are shown in Table 2.

In Table 2 the numbers N_L, N_D, and N_C refer to the number of measurements of L, D, and C. The quoted values of L, D, and C are the averaged results, all points more than three standard deviations from the mean having been discarded.

Several interesting things may be seen in these results: (1) The value of L, the distance to the subsidiary maximum in the large-cell AC curves, agrees quite well with that found in Section V*a* and with the spacing of the K-network to be discussed in Section V*c*. (2) The cell size D agrees very well with that FWHM measurements of Section V*a*. (3) If the horizontal velocity field has the previously assumed sinusoidal form, we would expect that[6] $L = 2D = 4C$. From Table 2 we find $D/L = 0.54$ and $D/L = 0.23$, indicating that even such a crude model as we have employed may contain some semblance of reality. In addition, *in every case* the cross-correlation tracings confirmed the odd parity of occurrence of maxima and minima described above.

TABLE 2

LARGE-CELL PARAMETERS AS DETERMINED FROM CROSS-CORRELATION CURVES

Case	$L(10^3$ km)	N_L	$D(10^3$ km)	N_D	$C(10^3$ km)	N_C
6/11/62	30 4±0 7	57	15 9±0 9	29	7 4±0 3	31
6/21/62	29 0±1 0	39	16 2±1 1	20	6 6± 4	28
6/23/62	31 8±1 1	46	17 3±1 1	28	7 3± 3	29
Total	30 8±0 6	142	16 5±0 6	77	7 1±0 2	88

So far we have not discussed the expected relative maximum at zero displacement for correlations at the center of the disk (Fig. 5). The significance of such a maximum is that it would directly indicate the existence of downward vertical motions at the cell boundaries and/or upward motions at the cell center, correlated with the chromospheric network.

On each of the three pairs of plates, four scans were made at the center of the disk. A typical tracing is shown in Figure 6, *b*. Note that a peak occurs at $x = 0$, in agreement with the schematic model (Figure 5, *b*, *right*). (The tilt of the tracing arises from gradual density gradients which could not be entirely compensated for.) The fields of view consisted of disks 0.5, 0.75, 1.0, and 1.25 cm in radius. Each of these twelve CC runs exhibited a maximum. However, the height of the maximum, expressed as a percentage change in the transmission through the two plates, ranged between 0.08 and 0.6 per cent, which shows why these maxima were difficult to see visually. Indeed, they were so small that one would normally tend to regard them as being due to random noise fluctuations, except for one very important property which all but one of these maxima possessed: They occurred not more than 0.1 mm from the position at which the two plates were in perfect registration;[7] i.e., at $x = 0$, exactly as predicted. This strongly suggests that the center-of-disk maxima at $x = 0$ are not merely spurious fluctuations, but really indicate that small vertical velocities do indeed exist in the large cells. This tends to confirm the weak evidence seen in the microphotometer tracings and AC functions described in Section V*a*.

[6] This is true for a rectangular-cell-plan form. For a circular-plan form, the ratio D/L is not 0 50, but 0.57.

[7] A distance of 0.1 mm on the 3.38-cm image corresponds to about 1700 km on the Sun.

© American Astronomical Society • Provided by the NASA Astrophysics Data System

1964ApJ...140.1120S

c) Spatial Periodicity of the Ca^+ Network

The existence of a coarse polygonal network pattern in spectroheliograms taken in the K_{232} core of Ca^+ was first reported by Deslandres (1899), and has been discussed by numerous authors since that time. Close inspection of this network structure quickly reveals two features: (1) There is a large spread in the sizes of the polygon "diameters" or "mesh widths," which, for example, Rogerson (1955) measured as 25000–70000 km. (2) To speak of a "mesh width" at all is somewhat difficult, since most of the polygons are quite irregular in shape and, moreover, are usually fragmented, with one or more sides missing.

Yet the high degree of spatial correlation between the Ca^+ emission and the velocity cells, discussed in the previous section, and the very strong moiré effect observed when two corresponding Ca^+ spectroheliograms are displaced with respect to each other, strongly suggest some sort of characteristic size to the structure, and perhaps a quasi-regular spacing of the network cells.

Using the auto-correlation analysis procedure described in Paper I, two AC measurements were made of the network pattern. In the first of these, seven 17-cm images, taken at various positions within 0.2 Å of the 3934-line-center during the summer of 1961, were reduced in size to a diameter of 94 mm, so that the entire solar disk would fit into the 95-mm opening of the correlation machine plate holders. Using the circular scan drive, a series of auto-correlations was obtained for ten successive annular regions, each 5 mm wide. That is, all of these tracings were made parallel to the limb, at various radii. For the second study, six 17-cm 1962 plates were treated by the foreshortening-removal apparatus. Then two linear runs were made on each, at the center of the disk, one in a roughly N.-S. heliographic direction, the other E.-W.

Results from these two studies were consistent with each other, yielding FWHM values of 6000–10000 km, the smaller values coming from plates which were exposed with the spectroheliograph exit slit centered on K_{2v}. Since it is well known that there is much more fine mottling in K_{2v} than in K_3, we conclude that the 10000-km value obtained from K_3 plates is closer to the true thickness of the bright network pattern. Most of the AC functions also exhibited one or more secondary maxima, which usually indicates the presence of a periodicity in the observed field For each AC scan, we measured the distance L (the "meshwidth") to the first subsidiary maximum. The average value of L from the circular scans was $\langle L \rangle = (33.8 \pm 0.72) \times 10^3$ km; for the linear scans, $\langle L \rangle = (29.8 \pm 1.1) \times 10^3$ km. The distribution of L sizes is shown in Figure 7, *a* and *b*, together with a normal distribution curve corresponding to $\langle L \rangle$ and the standard deviation σ. These results thus seem to imply the existence of a regular network pattern in Ca^+ emission with a cell size or meshwidth L = 30000–35000 km.

The number and heights of the secondary maxima varied considerably from one curve to another, presumably because of the small area of the Sun included in each scan. In order to obtain a more representative auto-correlation curve, we combined many separate curves to produce a composite or average curve. We expected this curve to show a clear secondary maximum, and perhaps a series of them. However, such a composite curve, made from the circular scan data, failed to show the maximum seen in each of the individual cases. Evidently the spread in the individual L's was such that minima on some curves coincided with maxima on others, the net effect being to "wash out" the expected maximum at 30000–35000 km.

Superficially, the cancellation of subsidiary maxima might indicate that the K-network emission does not possess a periodic or ordered structure. However, a real periodicity is strongly suggested by the alternating high-contrast and low-contrast effects (moiré pattern) one observes as two corresponding K-plates are slid slowly over one another in the auto-correlation machine: When the plates are in register, one sees the network pattern in sharp detail. Then, focusing attention on some area including ten or

© American Astronomical Society • Provided by the NASA Astrophysics Data System

1964ApJ...140.1120S

twenty cells, one observes that the contrast and subjective sharpness of detail are greatly reduced when the plates are out of register by about 15000 km. A further motion of about 15000 km *increases* the contrast and sharpness. Continued relative motion of the two plates results in an alternation of low- and high-contrast until the plates are out of register by several per cent of the solar diameter.

We prefer an alternative interpretation of the result, namely, that there is actually a distinct regularity of structure in every local region, but that the characteristic spacing distance L varies from one region to another. Indeed, we can easily imagine that the cell spacing could depend upon latitude, or upon the strength of the large-scale magnetic field that happens to be present in the given area.

In Table 3 we have collected together the several different measures of the cell spacing L, and have combined them into a single average value. We find excellent agreement among the various methods. In this table, $L1$ and $L2$ refer, respectively, to the circular and linear scans discussed in this section, $L3$ refers to the large cell data of Section V*a*, $L4$ to the K-LC data of Section V*b*, and L_T to all measurements taken together. The σ_m refers to the standard deviation of the mean.[8]

[8] Note, however, that the dispersion of the various *distributions* is about 7×10^3 km.

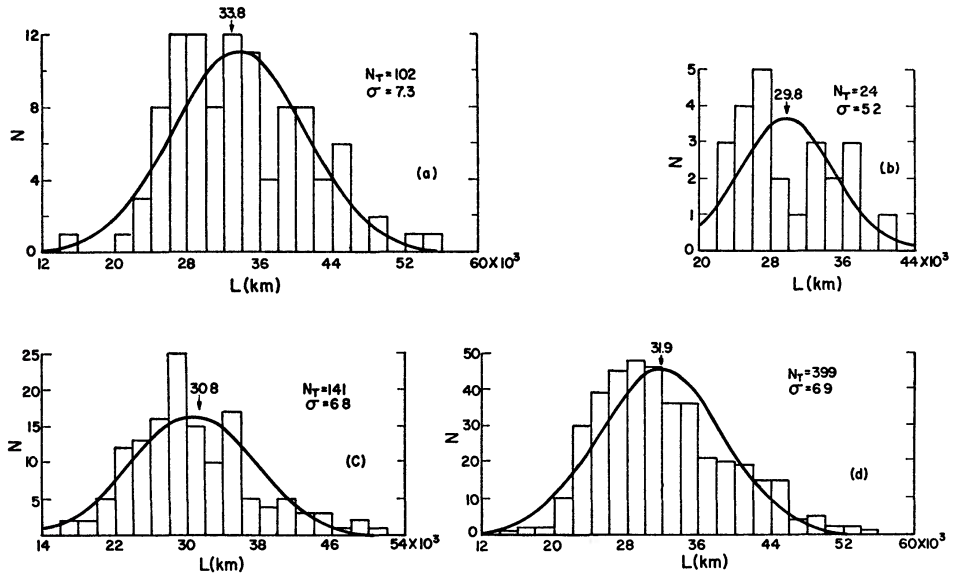

FIG. 7.—Distribution of cell sizes L from (*a*) circular scans of the Ca^+ network, (*b*) linear scans of the Ca^+ network, (*c*) CC curves of Ca^+ and large-cell plates, and (*d*) all four methods taken together

TABLE 3

SPACING OF LARGE CELLS

Case	$\langle L \rangle$ (10^3 km)	σ_m (10^3 km)	No of Measurements
$L1$	33 8	0 72	102
$L2$	29 8	1 07	24
$L3$	32 5	0 65	132
$L4$	30 8	0 57	141
L_T	31 9	0 35	399

© American Astronomical Society • Provided by the NASA Astrophysics Data System

1964ApJ...140.1120S

The distributions of sizes of $L1$, $L2$, and $L3$ have previously been shown in Figures 7, *a* and *b*, and 4. In Figure 7, *c* and *d*, we present the distribution of $L4$ and the composite L_T. The characteristic cell diameter from the combined methods is $L_T = (31.9 \pm 0.35) \times 10^3$ km.

Before leaving this section, we must consider the validity of interpreting the subsidiary maxima on AC curves as reflecting a real periodicity on the Sun. According to its mathematical definition, an AC function must be symmetric if the area of integration is indefinitely large. Thus any subsidiary maxima should occur in pairs; we shall call such AC curves "two-sided." In addition, if the network is strongly periodic, one might expect to find not only one pair of secondary maxima, but perhaps several. However, since we average only over a *limited* area, boundary effects may introduce asymmetries. As a result we find that our AC functions show maxima of various numbers and heights, and sometimes "one-sided" rather than "two-sided" maxima, or no secondary maxima at all. In Table 4 we summarize the measurements of first and second subsidiary maxima for cases $L1$, $L2$, and $L3$.

TABLE 4

SECONDARY MAXIMA OF LARGE-CELL AC FUNCTIONS

Case	No of 1st Maxima			No of 2d Maxima			Av No of Cells in Field of View
	2-sided	1-sided	0-sided	2-sided	1-sided	0-sided	
$L1$	44	14	3	22	15	24	130–170
$L2$	12	0	0	2	0	10	230–260
$L3$	59	13	6	7	10	61	70–90

Consider the number of first maxima. Only case $L2$, which had the best statistics, namely, a large rectangular field of view containing many more cells than $L1$ and $L3$, exhibited the ideal two-sided pattern for all runs. Also, referring again to the histograms of L sizes, one notices that the $L2$ size distribution is more narrow than that of $L1$ and $L3$. It will be recalled that in $L1$ and $L3$, annular integration areas were used including one narrow dimension usually 3–6 cell diameters wide. Only 70–80 per cent of these latter cases exhibit the symmetric pattern, implying that boundary effects may be affecting the result. This possibility seems even stronger when we look at the second maxima data. The $L2$ result suggests that the periodicity is not strong, since only two runs exhibited a second maximum. However, both of these were of the proper two-sided type. Both $L1$ and $L3$ showed considerably more second maxima, but almost as many of these were one-sided as two-sided, and thus should be viewed with suspicion.[9] Indeed, case $L1$ also showed a number of third, fourth, and fifth maxima, and even one run with a seventh-order maximum! But these higher-order maxima look very similar to small peaks on "noise" runs; i.e., cross-correlations of two unrelated Ca^+ plates taken some days apart.

To summarize this discussion, we conclude that on the Sun there exists a definite but somewhat weak local ordering of the emission structure seen on Ca^+ plates. The principal evidences of its existence are the high percentage of two-sided first maxima seen on auto-correlation curves, the moiré effect and K-LC correlation mentioned at the beginning of this section, and the excellent agreement among the average sizes $\langle L \rangle$ found

[9] It should be noted, however, that despite the possibility that these results may contain spurious effects, the average distance from eighty-three measurements of the second maximum is 57×10^3 km, very close to twice that obtained from the first maximum. The spread in sizes is again large, ranging from 32×10^3 km to 90×10^3 km.

© American Astronomical Society • Provided by the NASA Astrophysics Data System

1964ApJ...140.1120S

by the four methods $L1$, $L2$, $L3$, and $L4$. However, it is a weak effect, as indicated by the small number of tracings which show a symmetric second subsidiary maximum, the large spread found in individual L sizes, and the small height of the first subsidiary maximum, which is usually only 1–5 per cent that of the central maximum.

d) Lifetime of the Ca^+ Network

In order to obtain further information concerning the dynamics of supergranulation motions, it is of interest to measure the lifetimes of the velocity cells. However, to measure directly the velocity cell lifetime is difficult, since the cells become virtually invisible at the center of the disk, and thus can be observed only for a relatively short time, and only near the limb. Further, geometrical foreshortening is severe in the regions where the cells are visible, and cannot be adequately eliminated by the foreshortening-removal apparatus.

Having established in Section V*b* that the Ca^+ network and the large velocity cells are intimately related, it seems safe to assume that the lifetimes of these two phenomena must also be quite similar. Fortunately, the Ca^+ emission network is visible over the entire disk, so that individual elements could be followed for more than a week, if their

TABLE 5

LIFETIME OF THE K-NETWORK

Set	No of Plates	No of Correlations	Date (1962)	Image Size (cm)	Area on Sun (10^{10} km^2)	No of Cells	Maximum Δt
1	3	3	8/ 4–8/ 6	17	10 7	92	48^h54^m
2	8	17	8/21–8/23	8 4	9 3	80	43 53
3	4	12	8/31–9/ 1	8 4	6 2, 5 2*	53, 45*	24 6
4	2	1	9/23	8 4	28 3	244	4

* Correlations of two separate areas on these plates were made

lifetimes were that long. As mentioned in Section II, using the foreshortening-removal apparatus would permit almost distortionless viewing of a given element for just under 5 days; that is, for about 9–10 cm along the equator of the 17-cm image.

The lifetime of the bright Ca^+ flocculi (also called "coarse mottling" or "large chromosphere granules" by various authors) has been measured by Macris (1956, 1962), who visually followed more than 150 individual flocculi and recorded the percentage which remained as a function of time. In the present study, cross-correlation measurements were employed to measure the Ca^+ network lifetime. Some ambiguity exists between the terms "flocculi" and "network," so it is not certain whether Macris and the present work have measured lifetimes of the same or of different objects. De Jager (1959) has pointed out that the "fine mottles" cluster together to form the "coarse mottles" which in turn are often arranged in a "coarse network"; there are no sharp lines of demarcation among these groupings. In the present work we have measured an average lifetime associated with both flocculi and network emission, since the correlation machine responds to all intensity fluctuations in the field of view.

A total of seventeen plates in four sets was analyzed in this study. Table 5 lists the number of plates in each set, the number of correlations measured, inclusive dates of observation, image size, surface area on Sun in the field of view, number of cells in the field of view, and time interval between first and last plate of the set. The number of cells in the field of view was estimated as follows: On these plates 1 cm = 68×10^3 km ≈ 2 cell diameters, thus 1 cm^2 ≈ 4 cells. Since the Ca^+ network shows up almost equally well in K_{2v}, K_{2r}, and K_3, spectroheliograms taken at various wavelengths within $\Delta\lambda \approx 0.2$ Å

© American Astronomical Society • Provided by the NASA Astrophysics Data System

1964ApJ...140.1120S

of the line center were analyzed together. All the plates were processed in the foreshortening-removal apparatus before correlations were made. In addition, all "larger-than-network-size" emission regions and plages were masked out, so that only quiet areas remained in the field of view. Each pair of plates to be correlated was aligned by placing in register as many emission features as possible. Nearby sunspot regions (later masked out) proved very helpful in this regard. The lifetime of the K-network was measured in terms of the quantity $F(\Delta t)$, defined in equation (9).

From the seventeen plates, some thirty-three cross-correlations were made, with time intervals ranged from 4 minutes to 49 hours. All measurements utilized linear scans across the center of the disk ($\theta \leq 34°$). The results are shown in Figure 8. The lifetime T, defined as the length of time for the correlation to fall to e^{-1} of its initial value depends on the maximum time interval (t_m) used in the analysis. In Figure 8 two exponential decay curves are shown, one with $t_m = 20.3^h$, the other with $t_m = 48.9^h$. Several points are worth noting:

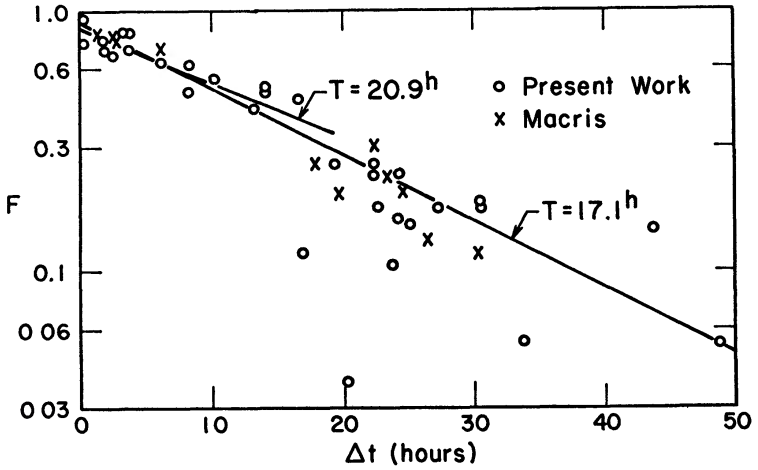

FIG. 8.—Lifetime of the Ca^+ network

1. T decreases considerably as t_m increases, as illustrated in Figure 9. This is understandable when one realizes both that the foreshortening removal is not perfect, and that as t_m increases, the network slowly changes shape, even though individual flocculi may remain; these two effects both tend to decrease F for large t_m, thus lowering T. It remains an open question what the "best" value of T is. We are inclined to choose the value $T = 19^h$–21^h, but if one chooses to include also the data with $t_m > 1^d$, one must assign a value $T \approx 17^h$.

2. The effect on the measured correlation due to fine mottling, photographic grain, small plate blemishes, etc., can be seen in Figure 8. One would expect from equation (9) that as $\Delta t \rightarrow 0$, F should go to unity. However, from the data analysis we find that the F-axis intercept is $F_0 \approx 0.82$. As an illustration, even for two spectroheliograms taken only 4 minutes apart, a Δt negligibly short relative to the network lifetime, the average value of F was 0.84. That is, small-scale solar details, which add to the height of an auto-correlation function, do not contribute significantly to cross-correlations, either because they disappear or shift in position (due perhaps to shorter lifetimes, local velocity fields, or very often due to changes in the local "seeing"). Similarly, photographic grain and tiny blemishes are impossible to mask out and also contribute more to auto-correlation heights than to cross-correlation heights.

To compare the present results with those of Macris (1962), we make the assumption than our F is equivalent to his per cent of flocculi remaining after a time Δt. After multi-

© American Astronomical Society • Provided by the NASA Astrophysics Data System

1964ApJ...140.1120S

plying his per cent data by 0.82 so that the two methods agree for $\Delta t = 0$, we have plotted his data together with ours in Figure 8. The agreement is excellent, and forms the basis for our earlier assertion that despite the differences in method and in terminology, we are essentially measuring the same phenomenon as Macris.

e) Correlation between Hα–Hβ Velocity Fields and the Ca+ Network

Spectroheliograms taken in the wings of the Balmer lines Hα, Hβ, and Hγ show a dark network pattern very similar to the *bright* Ca^+ network, a phenomenon first described by Deslandres (1910). For wavelength shifts of ±0.7 Å in Hα, ±0.4 Å in Hβ, and ±0.2 Å in Hγ, one finds the network pattern is at a maximum contrast. De Jager (1959) estimates the height of formation of these features to be about 1000 km above the photosphere. In this section we shall present the results of velocity measurements made in Hα and Hβ at the above wavelength shifts, and shall also show that the pattern of the hydrogen network coincides with that of the Ca^+ emission.

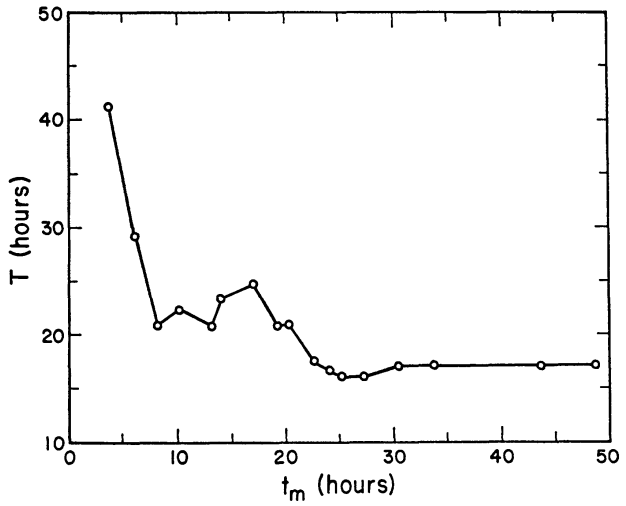

FIG. 9.—Dependence of Ca^+ lifetime (T) on maximum time interval (t_m) in the CC analysis

A total of forty-nine microphotometer tracings were made on Hα and Hβ Doppler plates, taken near the center of the disk, and the velocities in the network were measured. Figure 10, *d*, of Paper I is a typical example of such plates and illustrates the predominantly downward motion which characterizes the network. The average velocity is $-(1.2 \pm 0.2)$ km/sec relative to the quiescent background, with a few features reaching velocities of −2.0 km/sec (minus sign indicates receding line-of-sight velocity). No significant difference in the velocity-field structure was observed between the Hα and Hβ network. These velocity measurements are in excellent agreement with those of other authors, using different observing techniques. De Jager (1957, 1961*a*) has measured displacements of the Hα line which correspond to an average velocity of −1.1 km/sec, while Ca^+ K_3 velocities have been determined by St. John (1910) and Stepanov (1960), who found predominantly downward motions in flocculi averaging −1.1 km/sec and $-(1.7 - 2.3)$ km/sec, respectively.

To compare the spatial distribution of the downward-flowing hydrogen network and the bright Ca^+ network, we cross-correlated one Hα and two Hβ plates against Ca^+ photographs. In terms of a normalized cross-correlation coefficient F similar to that defined in equation (9), we measured an average correlation $F = 0.4$. Although this figure seems rather small at first glance, it actually implies a very high degree of correlation as is

© American Astronomical Society • Provided by the NASA Astrophysics Data System

1964ApJ...140.1120S

obvious to an observer comparing such plates by eye. It will be recalled from Section V*d* that it is very difficult to obtain an F-value higher than 0.8 even if a perfect one-to-one correspondence is expected. This would raise the measured correlation to $F \approx 0.4/0.8 \approx 0.5$. Two other effects which tend to decrease F are the time intervals (37–103 minutes) between exposures of the correlated plates, and the fine mottling and other "noise" which add appreciably to heights of auto-correlations but not to cross-correlations. We could easily believe that the true solar correlation is somewhat higher than 0.5. However, it is clearly not a perfect one-to-one correspondence. We pointed out at the beginning of Section V*c* that the Ca^+ network has a very fragmented appearance. This remark applies even more to Hα and Hβ velocity spectroheliograms, on which the descending material often seems to funnel downward at isolated points, these points being aligned so as to form the outline of a network pattern. Thus, though the outlines of the Ca^+ and Hα networks correspond closely, they differ considerably if one tries to match individual small features. Because of the general correspondence we conclude that the hydrogen velocity network, in addition to the Ca^+ network, occurs at the boundaries of the supergranules.

f) Correlation between Magnetic Fields and the Ca^+ Network

That there exists a close spatial correspondence between Ca^+ plages and BM regions was first observed by the Babcocks (1955). Their work was later extended by the more detailed measurements of Howard (1959), Leighton (1959), and Stepanov and Petrova (1959), who qualitatively found a virtual one-to-one spatial correspondence between Ca^+ emission and magnetic fields (henceforth called "K-M correlation").

Although the K-M correlation is clearly apparent to the eye when looking at the figures in those articles, no quantitative statistical analysis of this correspondence has been attempted for field strengths less than 5 gauss, in quiet areas on the Sun. (Stepanov and Petrova's study dealt mainly with higher field strengths in active regions.) In the present investigation, three different techniques were used in an effort to quantitatively measure the correlation at field levels below 5 gauss.

The first method was an attempt to extend the sensitivity of Leighton's apparatus to field strengths below 20 gauss. It was hoped that through the use of an improved beam splitter which transmitted more light and thus permitted narrowing the spectroheliograph slits, one might increase the Zeeman sensitivity of the apparatus. However this approach failed to increase the sensitivity enough to reach the 5-gauss level, mostly because the photographic noise level remained at least as high as in the earlier work.

The second method, carried out in collaboration with Howard, involved the magnetograph of the Mount Wilson Observatory and the technique that was described in Section III, wherein the K-line emission intensity and the magnetic field were monitored simultaneously. Using this technique, a series of scans were made near the center of the disk, separated from each other by 30″. Three such scans are shown in Figure 10. Figures 10, *a* and *b*, was obtained from scans made in a quiet positive UM region of the sun, where the Ca^+ emission occurs primarily in the network, while Figure 10, *c*, came from a scan through a small bipolar sunspot region. The magnetic field polarity is mainly positive (down on graph) in *a* and *b*, while it has both signs in *c*. On each part of the figure I is the dark noise level, II is the light-on noise level with the scanner stationary, while III and IV are the actual scans. It is seen that the noise level II is about 4 gauss, and therefore the method is quite successful in directly showing the K-M correlation if the field level is 5 gauss or larger. It should be noted that this was a preliminary and incomplete study; hence the absence of tracings made in negative UM regions, and the lack of a calibrated intensity scale for the Ca^+ emission. A more complete investigation is planned for the future.

In the third attempt to demonstrate the correlation below the 5-gauss level, a more detailed analysis was made of the polar region magnetograph tracings and Ca^+ spectro-

© American Astronomical Society • Provided by the NASA Astrophysics Data System

1964ApJ...140.1120S

heliograms obtained by Howard (1959). Using his tracings of September 3 and 5, 1958, magnetic contour maps were made at the 2-, 5-, 10-, and 15-gauss levels. The latter three levels resulted in contour maps essentially the same as those shown in Figure 4 of Howard's paper; new information was obtained only by addition of the 2-gauss contour. (It should be noted that due to a calibration error in the present work, the contour levels for the September 5 case were actually 1.5, 3.5, 7, and 11 gauss, somewhat smaller than had been originally intended.) In all cases, the measured levels were well above the noise level, which was less than 1 gauss. The two Ca^+ spectroheliograms were enlarged to the same scale as the magnetic maps, and black-on-white drawings made of the regions where K_{232} emission was visible.

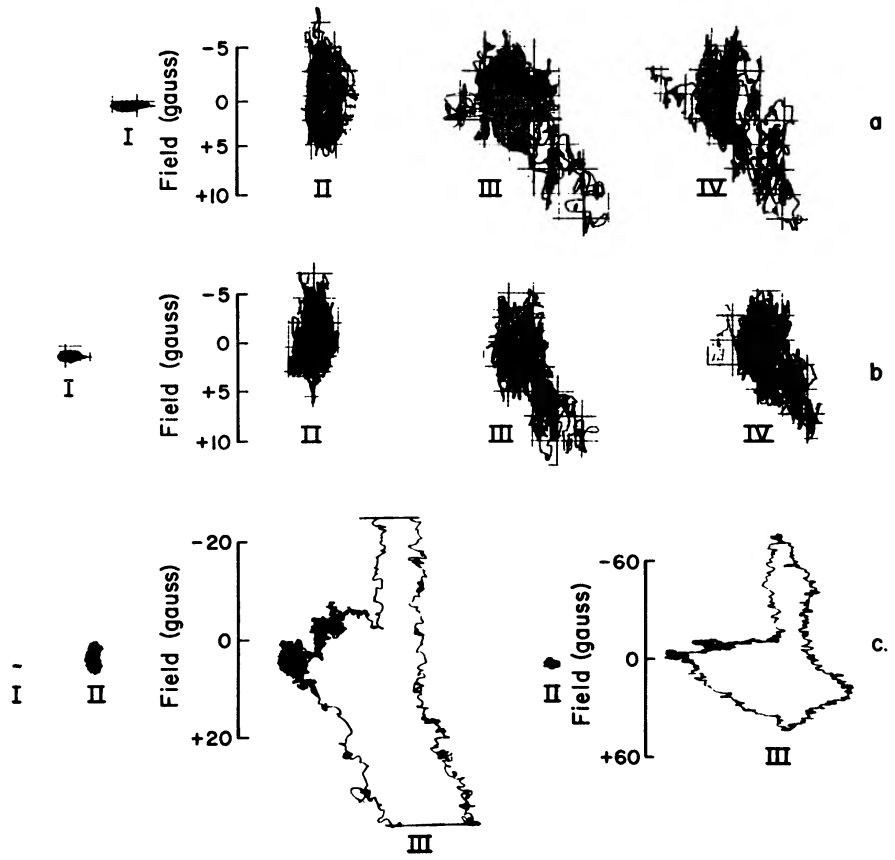

FIG. 10.—Actual X-Y recorder tracings of correlation between Ca^+ emission and magnetic field strength Motion of pen along horizontal axis indicates change in K_{232} intensity; motion in vertical direction indicates magnetic field variations. (*a*) (*b*) Tracings in quiet regions; (*c*) tracings across a small bipolar spot group.

A quantitative analysis of the K-M correlation was made in three stages, as follows:

1. From the tracings, a second drawing was made, showing only those regions having field strength $B \geq 5$ gauss. The K_{232} emission drawing and this magnetic field drawing were superimposed, as shown in Figure 11. The magnetic line tracing represents the center of each scan path; the slit width was actually equal to the separation between these lines. Each line segment on the magnetic field drawing was then given a value 4, 3, 2, 1, or 0, depending on whether it was completely covered by K_{232} emission, $\frac{3}{4}$ covered, etc. A line segment was considered to correlate with the K_{232} emission whenever it had a value 3 or 4, and to anticorrelate if the value was 0 or 1. Segments with value 2 were

© American Astronomical Society • Provided by the NASA Astrophysics Data System

1964ApJ...140.1120S

not counted. This procedure was carried out both when the two drawings were in proper alignment, and in three other "random" orientations, in essentially the same manner as the K-LC correlation discussed in Section V*b*. As before, the cumulative binomial probability distribution E was used to calculate the probability of finding the observed correlation as merely a random statistical fluctuation.

2. In the second stage of the analysis, drawings similar to the previous ones were made, with the added criterion that only those fields with $B \geq 10$ gauss were now included. The K-M correlation was measured exactly as in the previous case.

3. Since it is obvious that there must in general be a region of lower field strength surrounding a given contour line, it is expected that a certain amount of "artificial" correlation would exist between 2-gauss fields and the K_{232} emission, even if the "real" correlation were due only to fields greater than 5 gauss. Thus, before making the 2-gauss analysis, a new drawing was made, which included only fields in the range $2G \leq B < 5G$ (or, $1.5G \leq B < 3.5G$ for September 5). That is, all the high-level fields were removed.

TABLE 6

CORRESPONDENCE BETWEEN THE K-NETWORK AND MAGNETIC FIELDS

Field (gauss)	Date (1958)	Trials (N)	Successes (R)	R/N	P	$E(N; R, P)$
2 .	9/3	423	272	0 64	0 59	0 020
1 5	9/5	472	285	60	57	0 059
5	9/3	91	76	84	63	$1\ 7\times10^{-5}$
3 5	9/5	132	105	80	54	$5\ 6\times10^{-10}$
10	9/3	32	30	94	54	$1\ 3\times10^{-6}$
7	9/5	29	28	0 97	0 55	$6\ 5\times10^{-7}$

In addition, all of the Ca^+ emission which corresponded spatially with the strong magnetic field regions was similarly removed from the Ca^+ drawing. A small additional region surrounding the B = 5*G* contour line was also removed, to further reduce any remaining "artificial" correlation. It is hoped that by this method any correlations which still persist are really due to magnetic fields of less than 5 gauss. It should be noted that, due to the deletion of the high-field-strength regions, it was necessary to recalculate the correlations for the three random, non-aligned orientations of the two drawings. That is, any magnetic field segment which fell on top of the deleted region was thrown out, for to count it as an anticorrelated segment would have falsely lowered the probability E.

The results of this investigation are shown in Table 6. At the 5- and 10-gauss levels, in each case there is, roughly, only about one chance in a million of finding the observed correlation as a random statistical fluctuation. Note that about 95 per cent of the line segments correlated with the Ca^+ emission at the 10-gauss (7 gauss, September 5) level and 80 per cent at the 5-gauss (3.5) level. At the 2-gauss (1.5) level, only 60–65 per cent of the line segments correlated, and there remains a 2 (6) per cent probability that this weak correlation is due to chance. However, if we treat these two cases (September 3 and 5) as independent events, the probability that both correlations are merely random fluctuations is only about one in a thousand. Furthermore, there are several reasons to believe that the true correlation is higher than measured as will be discussed in the following section.

VI. DISCUSSION

a) Summary of Results

Since we have studied at some length a number of seemingly diverse phenomena, it seems appropriate at this point to briefly summarize these observations. First we described a system of atmospheric currents in the solar photosphere which manifest them-

© American Astronomical Society • Provided by the NASA Astrophysics Data System

1964ApJ...140.1120S

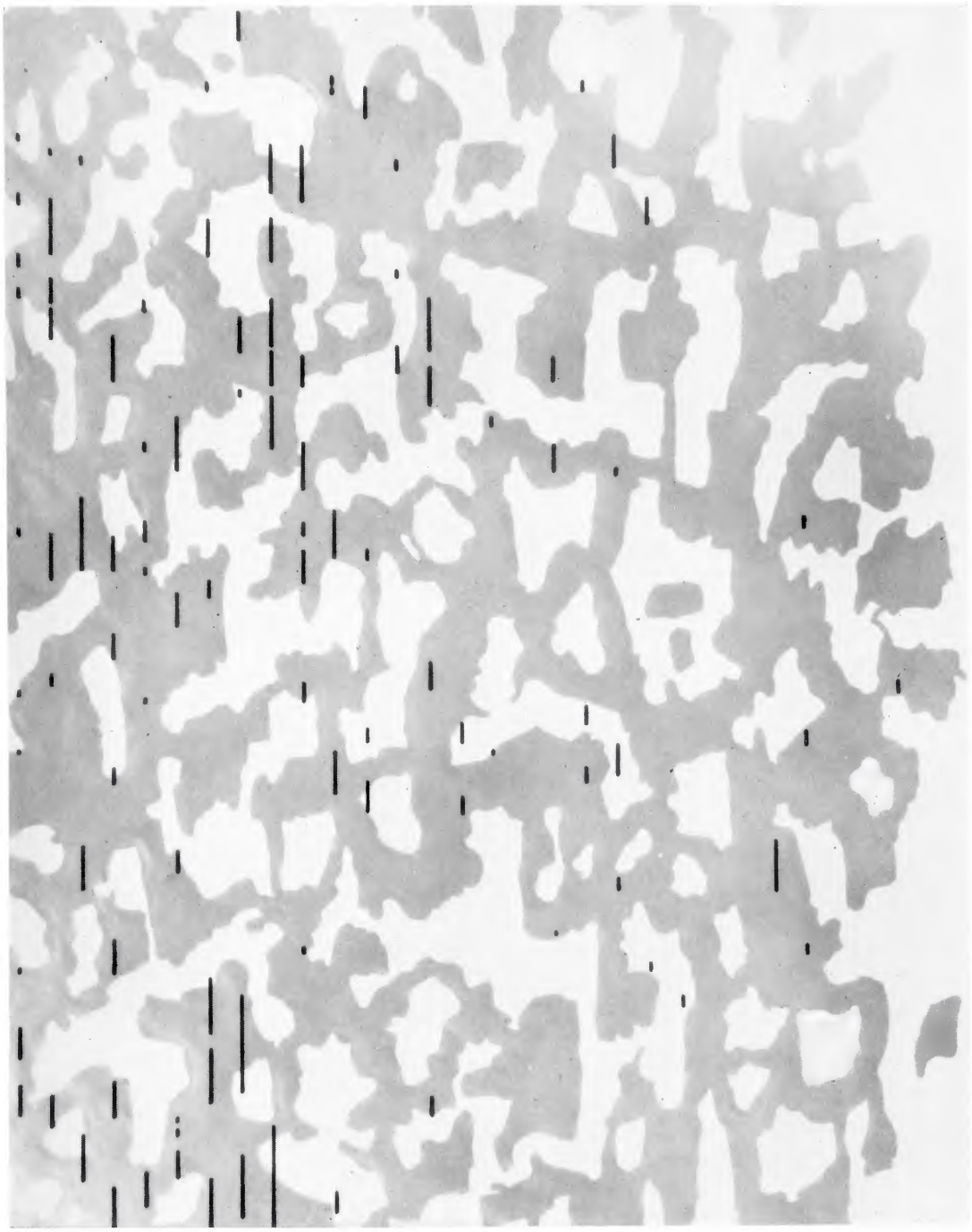

FIG. 11.—Superposition of Ca^{+} emission regions (gray areas) and magnetic field regions (black-line segments) having strengths $\geq$ 5 gauss. Data of September 3, 1958.

© American Astronomical Society • Provided by the NASA Astrophysics Data System

1964ApJ...140.1120S

selves as "large cells" with average diameters of 32000 km and lifetimes of 20 hours. These velocity cells exhibit mainly horizontal motions, the flow proceeding from the center of each cell toward the boundary with 0.4 km/sec average velocity. At any given time, there are roughly 5000 cells on the solar surface. Evidence was found for the existence of small vertical motions in the cells, the direction of the velocity being upward at the cell centers, and/or downward at the boundaries. The average magnitude of this vertical motion is probably about 0.1 km/sec.

Second, we measured correlations between the cells and three other phenomena: the chromospheric Ca^+ emission network, the downward-flowing $H\alpha$ and $H\beta$ network, and the 1.5–15-gauss magnetic field pattern. In each case the correlation showed that these phenomena occur mainly *at the boundaries* of the cells.

Four significant solar features seem to be clarified by the present observations:

1. The existence of a large-scale velocity structure in the photosphere is definitely established. Prior to the two-dimensional Doppler photographs described by Leighton (1961), only the spectrographic tracings of Hart (1954, 1956) had shown this structure, and her results had been challenged by Fellgett (1959) and others, who suggested that the secondary maxima in Miss Hart's "correlograms" were perhaps not truly solar phenomena but due to spurious effects. This controversy has now been resolved in Miss Hart's favor by our photographs, which strongly corroborate her work. Not only does Miss Hart's description agree with our conclusion that the distribution of cell sizes is very irregular, but also her peak velocities of 0.3–0.5 km/sec agree perfectly with our results. Two other studies of the large-scale velocity field have also recently confirmed our observations (Evans and Michard 1962; Howard 1962). The latter measured a power spectrum with a strong maximum in the 20×10^3–60×10^3-km wavelength region.

2. The observed horizontal motions provide a mechanism for building up relatively strong magnetic fields in a narrow network pattern, as is observed (Leighton 1959).

3. These magnetic "channels" in turn suggest an explanation for the origin of the Ca^+ emission network which has puzzled observers for seventy years since its discovery by Deslandres (1899), the bright emission network in the center of the $H\alpha$ line, and the dark network in the wings of $H\alpha$ and $H\beta$.

4. Further, the magnetic field probably guides the flow of ionized material and the propagation of magnetohydrodynamic (MHD) waves, which could thus account for the downward-flowing $H\alpha$, $H\beta$ network and the presence of spicules (Beckers 1963) in these regions.

We shall now discuss each of these four points in more detail.

b) Interpretation of the Observations

1. *The large cells as a convective phenomenon.*—The observed cellular flow pattern of the large-scale motions is strongly suggestive of convective motions, and we tentatively propose that we are dealing with a larger scale version of the familiar photospheric granulation—a "supergranulation." The observed dimensions of the large cells (32000 km) suggest that they originate in the Sun's convective envelope which extends from the bottom of the photosphere to depths of 5000–100000 km. Although the lifetime (20^h) of the supergranulation appears very long at first glance, if one considers the small velocity and the large dimensions one finds that the matter in all probability does not circulate more than once. This fact, coupled with the very irregular size and shape structure of the cells, suggests that we are observing an example of non-stationary convection, rather than the stationary laminar convection of classical Bénard (1901) cells. Since we are able to observe the supergranulation only from above, we have no means of determining the geometrical shape of the convection pattern; it may be either a circulating flow or a columnar convection such as a cloud or plume.

We may try to estimate the depth from which this convective motion originates by considering some examples. If D is the cell diameter, and H the depth, then the ratio

© American Astronomical Society • Provided by the NASA Astrophysics Data System

1964ApJ...140.1120S

$R = D/H$ is about 2–3 in the case of stationary Bénard cells. However, in non-stationary convection observed in nature, R is usually 5–10; this holds true over tremendous density and size ranges of at least 10^8! As examples, we refer the reader to Woodcock and Riley's (1947) observations of convection patterns in pond ice which had $R = 10$–30; to Tiros I satellite photos of cloud formations over oceans (Krueger and Fritz 1961) with $R \approx 10$; and to solar granulation[10] which has $R \approx 5$. In particular, the Tiros I photos show an amazing resemblance to the Ca^+ network pattern in the solar chromosphere. Thus for supergranulation diameters of 20000–50000 km, and assuming $R = 5$–10, we might expect a range of depths $H = 2000$–10000 km. As a second order-of-magnitude argument, it has often been observed that the lifetime T of a cell in non-stationary convection is given by $T \approx H/V$, where V is the average velocity of the rising currents. From our measured lifetime of 20 hours and assumed vertical velocity[11] of about 0.1 km/sec, we obtain $H = 7200$ km, in good agreement with the previous values.

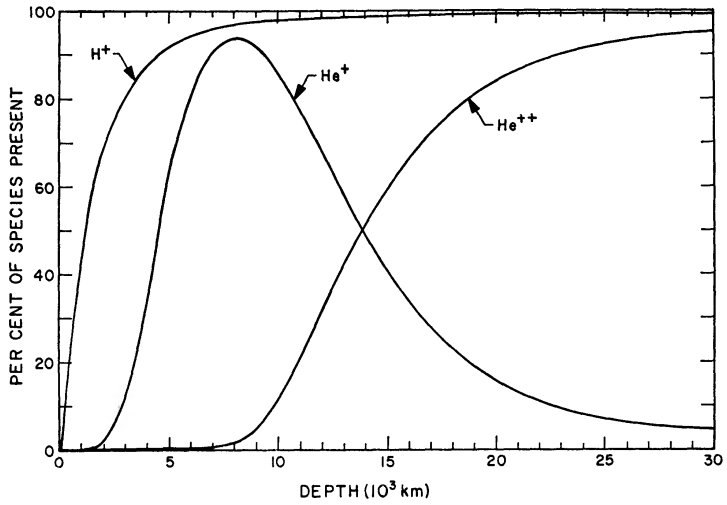

FIG. 12 —Ionization of hydrogen and helium in the convective envelope of the Sun. Depth is measured relative to optical depth 2/3 in the continuum. Unpublished data of Iben and Sears (1962).

In view of these considerations, it seems proper to ask whether there is any mechanism in the Sun which would select cell depths of roughly 5000 km. A possible answer lies in the ionization zones of either neutral He atoms or singly ionized He^+, or perhaps both. According to a solar model of Iben and Sears (1962), shown in Figure 12, these two regions begin at depths of about 2000 and 7000 km, respectively, which agrees very well with the above estimates. Zero depth in Figure 12 corresponds to optical depth $\frac{2}{3}$, approximately 300 km below the top of the photosphere. Note that Figure 12 also shows the hydrogen ionization zone which lies immediately below the photosphere. It is often argued that the hydrogen ionization may be partly responsible for the formation of the granulation because it produces a region with lower molecular weight lying below one of higher molecular weight, thus adding a secondary instability or perturbation to the already unstable convection region. A similar situation presumably exists for He ionization, and it might explain the supergranulation.

[10] In the case of the solar atmosphere we define H as the scale height at the granulation level (about 200 km), and compare this with the average granule diameter of perhaps 1000 km.

[11] This is our best estimate of the velocity at the photospheric level of our observations To satisfy the equation of continuity, the velocity must be smaller in the deeper layers, where the convection originates. This would lower the value of H somewhat.

© American Astronomical Society • Provided by the NASA Astrophysics Data System

1964ApJ...140.1120S

We next consider the regions of enhanced magnetic field strength, which appear to be caused by the large cell motions, and which, in turn, probably provide mechanisms for other observed phenomena.

2. *Magnetic regions due to large cells motions.*—In describing magnetic phenomena in the solar atmosphere, which contains sufficient ionized material to make magnetohydrodynamic effects important, one usually employs the parameter ν, defined as the ratio of the magnetic energy density $\beta = B^2/8\pi$ to the kinetic energy density $a = \rho v^2/2$. If $\nu \ll 1$, magnetic fields tend to be carried along with the mass motions, while if $\nu \gg 1$, the matter tends to be constrained by the magnetic lines of force. Near the top of the photosphere, where we observe horizontal cell motions of 0.4 km/sec and densities of 2×10^{-8} g/cc, we find that $\nu \approx 0.0025$ if we assume an average field strength of about 1 gauss. Such small fields would thus tend to be swept to the cell boundaries by the horizontal currents, and concentrate there in strengths several times greater than the average field. According to the above criterion it should be possible in these regions to constrain magnetic fields up to about 20 gauss. Parker (1963*a*, *b*), using kinematical hydromagnetic theory, and the observations described in Paper I, has predicted the concentration of magnetic flux sheets at the large cell boundaries, in excellent agreement with the order-of-magnitude arguments presented above. Let us compare these predictions with the observations. As we mentioned in Section V*f*, on the best Zeeman plates obtained by the photographic method (Leighton 1959), we often detect magnetic fields in the form of short lines or segments of a network pattern. Since these narrow regions are barely detectable, they must have field strengths comparable to the sensitivity of this method, namely, 10–20 gauss. Furthermore these enhanced field regions are sometimes so narrow that they are seen only on plates with excellent seeing. This indicates that the widths of the magnetic network in many cases may not exceed perhaps 1″ (≈ 700 km), which is approximately the best resolution obtainable with the 20-m tower telescope.[12] These results agree well with the observations of Howard (1962) and Kiepenheuer (1953). Howard, using an aperture about 2″ on a side, measured r.m.s. magnetic field fluctuations of 8 gauss, with peaks of 10–20 gauss occurring at distances of 20000–30000 km along his tracings. Kiepenheuer's earlier work had much poorer spatial resolution; however, he also found occasional "field patches" in the 10–20-gauss size. Under good seeing conditions he observed a fine structure in these patches, and speculated that this structure had dimensions not larger than 10″ or 20″, and that the field amplitudes might well exceed 20 gauss. Also we compare these results with our study of Howard's tracings described in Section V*e*. In this case, the aperture was 10″ on a side, and we found that a field level of about 2 gauss correlated well with the Ca^+ network. If the actual dimensions of the magnetic fine structure are really closer to 2″ on a side, we must correct these smeared-out observations, obtaining a field of roughly 50 gauss. The range of field strengths observed by these various techniques, namely, 10–50 gauss, is consistent with the limit imposed by the equipartition argument; i.e., that fields can be constrained by the material motion until $\beta \approx a$.

Another qualitative observation is worth mentioning before we leave this section. We often observe at the periphery of sunspot and plage regions that the patches of magnetic fields and Ca^+ emission tend to break up into a network pattern. In Ca^+ spectroheliograms the transition from solid plage to bright network to weak network is a smooth process as one follows the emission from the center of a sunspot outward into a quiet region on the solar surface. For examples of this behavior, refer to Figure 7, *b* and *c*, of Leighton's 1959 article. In addition, if one traces the life-history of a large sunspot region, many times one finds that as the spot group breaks up, the plage appears to disintegrate slowly into a network pattern. We infer from these observations that the

[12] Of course, the possibility exists, from an observational point of view, that we are seeing only smear-out fields due to our resolution limits, and that the actual fields are stronger and concentrated in even smaller regions.

© American Astronomical Society • Provided by the NASA Astrophysics Data System

1964ApJ...140.1120S

horizontal currents in the large cells may be slicing away bits of magnetic field from the edges of the sunspot, sweeping them to the cell boundaries, and then slowly dispersing this field from one cell boundary to another, into a continually expanding network pattern around the sunspot group.

To summarize these observations, it appears that the large-cell motions are closely connected with the localization of magnetic fields in the solar atmosphere, both by concentrating the weak average field into narrow network regions, and through the breaking up of concentrated sunspot fields into a widespread network pattern. We consider next some of the consequences of the existence of this "magnetic network."

3. *Origin of the Ca^+ and hydrogen networks.*—The fine network of relatively strong magnetic fields formed by the large-cell motions is presumed to extend upward into the chromosphere, and there forms the basis for the Ca^+, Hα, and Hβ networks, as follows: Osterbrock (1961) has shown that enhanced heating of the chromosphere occurs in those regions where magnetic fields exist. Therefore, we expect the network structure to be at a higher temperature than the surrounding material. According to the theory of K- and Hα-line formation summarized by de Jager (1959), this is exactly the condition required to explain the bright network in the cores of the K- and Hα-lines, and the dark network in the wings of Hα (and Hβ). That is, theoreticians previously had correctly predicted higher temperatures in the network regions, but were unable to discover a mechanism for producing these increased temperatures. The present observations of the strong spatial correspondences between Ca^+ emission and velocity cells, Ca^+ and magnetic fields, and Ca^+ and the Hα, Hβ velocity networks, coupled with Osterbrock's calculations, seem to provide the missing link in explaining the origin of the chromospheric network. We conclude that the Ca^+ network is not due to a circulation of matter in the chromosphere as suggested by Deslandres (1910) and Wasiutynski (1946), but due to a more general circulation which *underlies* the chromosphere.

Two more points are worth mentioning. First, we would expect that the contrast between network and background should be a maximum in the region of highest energy dissipation. Osterbrock finds that for fields between 2 and 50 gauss, maximum dissipation occurs at chromospheric heights of 500–2000 km, which is in excellent agreement with the heights where the dark Hα, Hβ network is most clearly seen.

Second, the magnetic lines of force will diverge as they extend higher into the chromosphere as the matter density decreases, which might explain the larger FWHM (10000 km) of the Ca^+ network at a height of about 4000 km, compared to the Hα, Hβ network at 1000 km, which has a FWHM of only 5000 km. Further, both of these widths are much larger than that of the photospheric magnetic fields, which are barely resolvable under the best seeing conditions, and thus generally not over 1000–2000 km in size.

The magnetic network and its relation to the Ca^+ network is shown in Figure 13. The upper figure is a Ca^+ spectroheliogram showing the network obtained in K_{2v}, the middle shows the magnetic network, while the lower picture is a print of one of the original Ca 6103 spectroheliograms from which the magnetic record was made. It is seen that not a single sunspot is present.

Finally, we turn very briefly to the enhanced flow of ionized material and MHD wave propagation due to the magnetic network.

4. *Magnetic influences on chromospheric velocities.*—At the level of the large cells, we found that the ratio ν of magnetic to kinetic energy density was much less than unity. However, in the chromosphere where we observe the Hα, Hβ, and Ca^+ networks we find that $\nu > 1$. Let us suppose that the concentrated fields at the cell boundaries are on the order of 10 gauss. Then de Jager's values (1961*b*) for the densities at 1000 km (Hα, Hβ) and 4000 km (Ca^+), namely, 8×10^{-11} and 10^{-13} g/cc, respectively, lead to ratios $\nu = 2.5$ and $\nu = 2000$, if we assume $v = 2$ km/sec. Thus at both heights ionized material can be trapped by the magnetic network. Since some of the hydrogen and most of the

© American Astronomical Society • Provided by the NASA Astrophysics Data System

1964ApJ...140.1120S

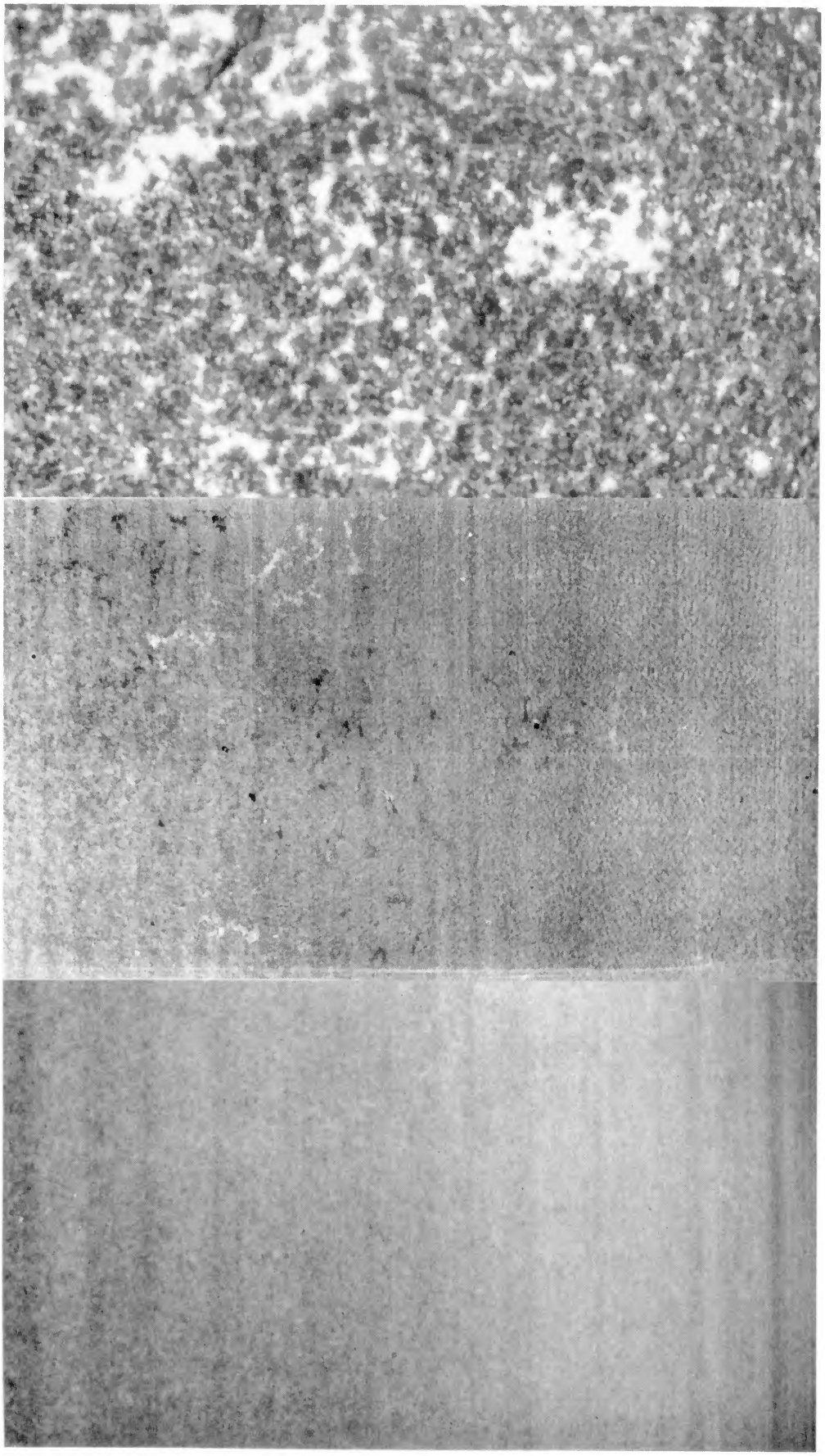

FIG. 13.—Spectroheliograms of July 18, 1962, showing details of Ca^+ and the magnetic network. *Top:* Ca^+; *middle:* magnetic features; *bottom:* an original Ca 6103 spectroheliogram.

© American Astronomical Society • Provided by the NASA Astrophysics Data System

1964ApJ...140.1120S

metals at these chromospheric levels are ionized,[13] we would expect the matter to move more freely along the lines of force. If one accepts a chromospheric and coronal model in which matter is carried to high levels by various eruptions such as flares and spicules then it seems reasonable that much of this excess material will slowly fall back down into the lower atmosphere. This descending, partly ionized gas should therefore funnel down along the lines of force concentrated above the cell boundaries, resulting in the descending network seen in the wings at Hα and Hβ.

It seems quite possible that small rising spots which we see at the edges of the falling Hα, Hβ network are spicules seen on the disk. This phenomenon, also, can be explained by the enhanced magnetic fields in this network region, if we accept Osterbrock's (1961) interpretation of spicules as slow-mode disturbances carrying chromospheric material up along the magnetic lines of force into the corona.

c) Conclusion

Before closing we should mention two areas which did not yield completely satisfactory results and in which further observational work would be desirable. The first of these is the correlation between the Ca^+ emission and the magnetic network. Although the measured K-M correlation below 5 gauss appears to be real and positive, it was certainly not a one-to-one correlation. However, the observational difficulties were such that the true solar correlation is certainly much larger than our value, and might actually be one to one. Many correlation-destroying effects were present in our observing techniques which tended to lower the measured correlation. These included poor seeing, the long time (about 2 hours) needed to complete the magnetic tracings (during which both solar rotation and finite cell lifetime produce an artificial anti-correlation), the large aperture used in the magnetograms (about 7000 km on a side) which "smeared out" small-scale features, the use of drawings of the Ca^+ network (which were subject to the observer's judgment concerning the extent of the emission region) and line drawings for the magnetic field regions, close proximity of the solar limb to the measured regions with resultant foreshortening distortions, and finally, the fact that the magnetic measurements were made in a photospheric line, while the Ca^+ emission probably originates some 3000–4000 km higher in the atmosphere, where the lines of force are more spread out (due to the lower density), and thus the apparent size of the magnetic field region may be much smaller than the dimensions of the Ca^+ emission.

Unfortunately, it is not possible at present to make a two-dimensional map of the magnetic field regions using the very small (2″) apertures described in Howard's 1962 paper, since there is no way of guiding the solar image accurately enough. This may become feasible in the near future, and seems very necessary. In the meantime, improvement in the sensitivity of the X-Y recorder technique so that smaller apertures can be used, would yield valuable information on the K-M correlation. This method has the great advantage that both channels of the recorder simultaneously see the same spot on the solar surface; the correlation is made automatically without need for elaborate drawings, enlargements, superposition of images, and other intermediate steps in the laboratory. The preliminary observations of 1962 used an aperture of 10″ × 18″, clearly too large to properly analyze a network pattern which may be only 1″–2″ wide.

The second area needing more data is the matter of vertical motions in the supergranulation. Although evidence for such motions was found by four different methods, which gives us some confidence in the result, more work needs to be done. At least three effects cause considerable difficulty in observing the vertical motions. First, these motions may really be so small that they are difficult to resolve by the Doppler photographic technique. Second, they may be hidden by the turbulence in the mushrooming top of

[13] According to van de Hulst (1953), at the bottom of the chromosphere, only one hydrogen atom in 10^6 is ionized. But the fraction of protons increases rapidly with height, and becomes equal to the neutral atoms at a height of 4000–5000 km.

© American Astronomical Society • Provided by the NASA Astrophysics Data System

1964ApJ...140.1120S

the convection plume. Third, they may be masked by the small-scale vertical oscillations. Thus it would be worthwhile to investigate other methods of approaching this problem. For example, it may be possible that the large cells could be seen superimposed on the small-scale granulation: Close inspection of high resolution granulation photos shows not only a scattered number of dark "pores," but also a very fragmentary system of dark, narrow "strips." Perhaps these dark holes and strips are regions either where the large cell vertical motion or the magnetic network is breaking through the granular surface. It will be recalled that numerous authors have reported secondary maxima at about 15000 km in auto-correlation studies of the small-scale granulation. This figure is close enough to supergranulation dimensions to suggest the presence of some features of the large cells. With respect to large-scale horizontal currents in the granulation reported by Janssen (1896), we agree with the conclusion of Hansky (1906) and Chevalier (1908) that Janssen's "photospheric net" was not a solar effect, but due to poor seeing, and thus there is at present no evidence for large-scale horizontal motions in the granulation outside of sunspot regions. Of course this is also apparent from inspection of the magnificent Stratoscope I photographs (Bahng and Schwarzschild 1961; Schwarzschild 1959; Danielson 1961), in which atmospheric seeing problems have been virtually eliminated. None of these show any distortions of the granular pattern which might be due to large-scale horizontal velocities.

Earlier in the discussion we suggested that the gradual disintegration of sunspots might be due to "erosion" of the penumbral boundaries by the large cell currents. Not only this aspect of possible sunspot–large-cell relations needs further study, but also the following idea: Perhaps pores and sunspots are formed directly as the result of the circulation in the supergranulation. This could conceivably happen in either of two ways. First, it has been observed in the study of Bénard cells that small particles, swept to the cell boundaries by the horizontal currents, then flow *along* the boundary and pile up at the vertices of the polygonal cells. In analogy, if there is a weak magnetic field already present on the solar surface, then the large-cell motions might be expected to concentrate these fields at the polygon vertices, resulting in the small pores seen in granulation photos. The second method of sunspot genesis involves a different aspect of the large-cell motions, and results in sunspot formation at the cell centers. It may be that sunspots are the consequences of strong deep-lying magnetic fields which are carried up from below by a rising plume of gas. The well-known Evershed effect may give some credence to the second hypothesis. At the photospheric level, penumbral velocities are directed radially outward from the umbra, and thus look very much like the large-cell motions. Both of these ideas are rather speculative, but might deserve detailed study.

Finally, it is hoped that the observations reported in this paper will stimulate theoretical studies which may explain more satisfactorily the true origin and nature of the convective supergranulation. A recent model of the hydrogen convection zone by Böhm (1963) predicts the existence of horizontal velocities at the top of the convection zone, extending into the low chromosphere, in qualitative agreement with the present observations. However, Böhm's model predicts a continuous spectrum of wavelengths, whereas we observe a definite peak in the size distribution at about 30000 km, with no evidence that the supergranulation is merely the tail end of a spectrum which includes the small-scale granulation as well. It would appear that further theoretical analysis is still needed to resolve some of these questions.

We wish to thank Dr. R. Howard for his assistance with the magnetic observations, for the use of his 1958 data, and several discussions. We are grateful to Dr. E. Spiegel for a very helpful discussion, and to Mr. Gary O. Fitzpatrick for help with observations and data reduction. One of us (G. W. S.) wishes to thank the Hughes Aircraft Company and Space Technology Laboratories for fellowships during the course of this investigation.

© American Astronomical Society • Provided by the NASA Astrophysics Data System

1964ApJ...140.1120S

REFERENCES

Babcock, H W., and Babcock, H D. 1955, *Ap. J*, **121**, 349.
Bahng, J., and Schwarzschild, M. 1961, *Ap. J.*, **134**, 312.
Beckers, J 1963, *Ap. J*, **138**, 648.
Bénard, H. 1901, *Ann. Chim. Phys.*, **23**, 62.
Böhm, K. 1963, *Ap. J.*, **137**, 881.
Chevalier, S. 1908, *Ap. J.*, **27**, 12.
Danielson, R., 1961, *Ap. J.*, **134**, 275.
de Jager, C. 1957, *B.A.N.*, **13**, 133.
———. 1959, *Hdb. d. Phys*, ed. S. Flügge (Berlin: Springer-Verlag), Vol. **52**.
———. 1961*a*, *Colloq Astrofis.* (*Suppl. Mem. Soc. Astr. Ital.*), No. 3, p 73.
———. 1961*b*, Vistas in Astronomy, **4**, 143.
Deslandres, H. 1899, *C.R.*, **129**, 1225.
———. 1910, *Ann. Obs. Astr. Phys. Paris*, **4**, 116.
Evans, J., and Michard, R. 1962, *Ap. J.*, **136**, 493.
Fellgett, P. 1959, M.N., **119**, 475.
Giovanelli, R., and Jefferies, J. 1961, *Australian J. Phys*, **14**, 212.
Hansky, A. 1906, *Bull. Soc. Astr. France*, Vol. **23**.
Hart, A. 1954, *M.N.*, **114**, 17.
———. 1956, *ibid.*, **116**, 38.
Howard, R. 1959, *Ap J.*, **130**, 193.
———. 1962, *ibid.*, **136**, 211.
Hulst, H. van de 1953, *The Sun*, ed. G. Kuiper (Chicago: University of Chicago Press), chap v.
Iben, I., Jr., and Sears, R. 1962, unpublished.
Janssen, J. 1896, *Ann. Obs. Astr. Phys. Paris*, **1**, 103.
Kiepenheuer, K. 1953, *Ap. J.*, **117**, 447.
Krueger, A., and Fritz, S. 1961, *Tellus*, **13**, 1.
Leighton, R. 1959, *Ap. J.*, **130**, 366.
———. 1961, *Nuovo Cimento Suppl.*, **22**, 321.
———. 1963, *Ann. Rev. Astr. Ap.*, **1**, 19.
Leighton, R., Noyes, R., and Simon, G. 1962, *Ap. J.*, **135**, 474.
Macris, C. 1956, *Rend. Accad. naz. Lincei Roma VIII*, **21**, 303.
———. 1962, *Mem. Soc. Astr. Ital.*, **33**, 85.
Noyes, R., and Leighton, R. 1963, *Ap. J.*, **138**, 631.
Osterbrock, D. 1961, *Ap. J.*, **134**, 347.
Parker, E. 1963*a*, *Ap. J.*, **138**, 226.
———. 1963*b*, *ibid.*, p. 552.
Pellew, A., and Southwell, R. 1940, *Proc. Roy. Soc. London, A*, **176**, 312.
Rogerson, J , Jr. 1955, *Ap. J.*, **121**, 204.
St. John, C. 1910, *Ap. J.*, **32**, 36.
Schwarzschild, M. 1959, *Ap. J.*, **130**, 345.
Simon, G., and Leighton, R. 1963, *A.J.*, **68**, 291.
Stepanov, V. 1960, *Izv. Krims. Ast. Obs.*, **23**, 184.
Stepanov, V., and Petrova, N. 1959, *Izv. Krims. Ast. Obs*, **21**, 152.
Wasiutynski, J. 1946, *Ap. Norvegica*, **4**, 143.
Woodcock, A., and Riley, G. 1947, *J. Meteorol.*, **4**, 100.

© American Astronomical Society • Provided by the NASA Astrophysics Data System